Industrial Crops & Products 226 (2025) 120614

Contents lists available at ScienceDirect

Industrial Crops & Products

journal homepage: www.elsevier.com/locate/indcrop

Comparisons of alkali, organosolv and deep eutectic solvent pre-treatments on the physiochemical changes and lignin recovery of oak and pine wood

Yujie Mao [a], Ilayda Tarhanli [b], Gwyn Owen [a], Chai Siah Lee [a], Erkan Senses [b,*], Eleanor Binner [a,*]

[a] Faculty of Engineering, University of Nottingham, University Park campus, Nottingham NG7 2RD, United Kingdom
[b] Chemical and Biological Engineering, Koc University, Sariyer, Istanbul 34450, Turkey

ARTICLE INFO

Keywords:
Lignocellulosic biomass
Pre-treatment
Deep Eutectic Solvents
Microwave-assisted extraction
Delignification
Physiochemical property

ABSTRACT

Pre-treatment is a crucial and the most energy-intensive step for successful valorisation of lignocellulosic biomass in a biorefinery. This study provides systematic comparisons of the biomass fractionation and physiochemical changes of oak and pine wood waste using three pre-treatment methods: 1). an alkali process (2.5 M NaOH and 0.4 M Na_2S), 2). an Organosolv process (70 % ethanol in water with 1 % w/w H_2SO_4), and 3). an emerging Deep Eutectic Solvent (DES) process (p-Toluenesulfonic acid: Choline Chloride: Glycerol in 2:1:1 molar ratio). Among the three pre-treatments, DES exhibits the highest process efficiency, achieving a solid residue weight loss of 43.5 % (oak) and 35.3 % (pine) corresponding to the highest delignification yield of 66.1 % (oak) and 79.2 % (pine) at a much shorter time (30 min vs 180 min) and less energy consumption (1/5 to 1/8) than alkali and Organosolv. DES-treated wood shows higher sensitivity to thermal degradation at lower temperatures, indicating better potential as a solid fuel. It also shows a lower degree of crystallinity of 28.6 % (oak) and 26.7 % (pine) and higher phenolic content, suggesting potentially better enzymatic susceptibility during bioconversion. On the contrary, Organosolv-treated wood presents preserved crystallinity of 41.6 % (oak) and 35.5 % (pine) and macro-/nano-structures, indicating potentially better mechanical properties for functional materials. It is hoped that this study will provide insights to informing sustainable solvent selections in biorefinery and biomass product development for value-added applications.

1. Introduction

The adverse environmental impacts of fossil fuels and petrochemicals, as well as concerns over energy security, necessitate the development of renewable feedstocks. Lignocellulosic biomass (LCB) is a renewable, relatively carbon-neutral resource of energy that is readily available, with a yearly supply of approximately 200 billion tonnes worldwide. Furthermore, it is not edible and thus does not interfere with food and feed supplies (Kumar et al., 2018). The main constituents of LCB are cellulose (30–50 %), hemicellulose (20–30 %), and lignin (15–30 %) (Wang and Lee, 2021), which together form a complex and rigid 3-dimensional structure contributing significantly to the biomass resistance to microbial and/or enzymatic deterioration (Loix et al., 2017).

Over the past decades, cellulose and hemicellulose, which are polysaccharides, have been proven as promising sources of a broad spectrum of bioproducts ranging from biofuels and specialty chemicals (e.g. ethanol, butanol, and furfural) to functional materials (e.g. bionanomaterials) (Lobato-Rodríguez et al., 2023; Ning et al., 2021). Lignin, as an aromatic polymer, cannot be valorised through the same routes, and in fact its presence as a recalcitrant layer covering cellulose and hemicellulose in the LCB reduces the production efficiency of those biochemicals (Devi et al., 2022). Therefore, a pre-treatment step is often required to break down the recalcitrant structure of the LCB, delignifying it and making it more susceptible to chemical, thermal and biological upgrading (Ning et al., 2021). Other requirements of the pre-treatment techniques include cost-efficiency, environmental sustainability, and practicability for process scale-up and commercialisation (Wang and Lee, 2021).

The commercial pre-treatment method for delignification is the Kraft process, which has been developed from the pulp and paper industry for the conversion of wood into pulp (paper) since 1890. In this process, LCB

* Corresponding authors.
E-mail addresses: Yujie.Mao1@nottingham.ac.uk (Y. Mao), itarhanli16@ku.edu.tr (I. Tarhanli), enygo1@exmail.nottingham.ac.uk (G. Owen), chai.lee@nottingham.ac.uk (C.S. Lee), esenses@ku.edu.tr (E. Senses), Eleanor.Binner@nottingham.ac.uk (E. Binner).

https://doi.org/10.1016/j.indcrop.2025.120614
Received 20 November 2024; Received in revised form 23 January 2025; Accepted 25 January 2025
Available online 7 February 2025

is treated by a hot alkaline mixture of sodium hydroxide (NaOH) and sodium sulfide (Na2S). The range of process conditions of Kraft process is variable (usually at temperatures from 145–170 °C and time from 2 to 3 h) (Pola et al., 2022; Woiciechowski et al., 2020), depending on many factors such as the biomass types, solvent concentrations and targeting product requirement (Lahtinen et al., 2021). This pre-treatment breaks the ether bonds between the cellulose and the lignin fraction, with cellulose preserved for further processing to make paper and fragmented lignin solubilised into alkali water, resulting in a huge volume of black liquor (Haq et al., 2020). However, the pitfalls associated with the Kraft process include the use of corrosive solution and the generation of large quantities of wastewater causing corrosion to the equipment unit and adding extra cost for solvent disposal (Vidal et al., 2021). Additionally, due to the high sulphur content from the Kraft solution, Kraft lignin also has more sulphur impurities in its structure such as covalent bonding with aliphatic thiol groups, which deactivate its chemical functionality and cause an unpleasant odour, which may limits its potential application (Chio et al., 2019; Kumar et al., 2020).

The Organosolv method is another common pre-treatment. Some examples of the most commonly used organic solvents are ethanol (Liu et al., 2020; Parot et al., 2022), acetone (Luo and Abu-Omar, 2018), methanol (Luo and Abu-Omar, 2018; Ouyang et al., 2018) and ethylene glycol (Wei et al., 2021) mixed with water in various percentages, and usually coupled with a small addition of acid (Ouyang et al., 2018), alkali (Wei et al., 2021) or salts (such as ferric chloride ($FeCl_3 \cdot 6H_2O$)) (Parot et al., 2022). However, efficient delignification by the Organosolv method often requires a hydrothermal temperature at 160–200 °C (associated with high pressure concerns (e.g. the saturated pressure for ethanol at 180°C reaches 22.9 bar)) for at least 2 hrs to reach approximately 60 % delignification yield (Liu et al., 2020; Parot et al., 2022). for at least 2 hrs to reach approximately 60 % delignification yield (Liu et al., 2020; Parot et al., 2022). Although many efforts have been made to develop and improve Organosolv processes using the experimental setups, due to the challenges such as high solvent cost and high energy consumption, the commercialisation of these processes on the industrial scale is still limited (Rabelo et al., 2023).

There has also been increasing effort in developing novel and sustainable solvents for LCB pre-treatment, among which Deep Eutectic Solvents (DES) have attracted considerable attention. DES are defined as systems composed of a mixture of at least two components (i.e., Lewis or Brønsted acids and bases containing various anionic and/or cationic species besides other molecular compounds) in certain molar ratios that act either as hydrogen bond acceptor (HBA) or hydrogen bond donor (HBD), showing a decreased melting point of the system than that of each individual component (Lobato-Rodríguez et al., 2023). Advantages of DES include low vapour pressure, non-flammability, high chemical and thermal stability, and tailorability towards targeted biorefinery applications (Perna et al., 2020). DES also pose higher selectivity in lignin solubilisation, thus exhibiting potential benefits in preserving the cellulose and hemicellulose fractions for further upgrading to higher value-added applications (del Mar Contreras-Gámez et al., 2023; Lobato-Rodríguez et al., 2023).

Apart from the emerging of novel solvents, novel heating techniques such as microwave heating has been widely reported to accelerate or enhance the biomass biorefinery efficiency. Microwave heating poses advantages due to its unique selective heating mechanisms achieving quicker heating rates under microwaves than in conventional heating (González-Rivera et al., 2020), thus reinforcing pre-treatment performance in a reduced heating time while minimising the thermal degradation of bioactive compounds (Mao et al., 2021). Microwave can also penetrate throughout the whole volume of the bulk material, overcoming the heat and mass transfer limitations during conventional heating (Patil and Rathod, 2023) while offering precise temperature control and uniform heating (Zou et al., 2023).

Although much progress has been made in developing various conventional and novel pre-treatment methods for lignin removal and LCB conversion, there lacks systematic and comprehensive comparison on the influence of various pre-treatment methods on the structural properties of the resulting biomass residue obtained from different methods, and this limits understandings of the potential upgrading routes. Rahman et al. (2024) investigated the alkali process (12 % NaOH and 25 % Na_2S, at 160–170 °C and 3 h) on the crystallinity structure, morphology and chemical changes of jute and banana tree fibres after delignification. Ouyang et al. (2018) proved the increased enzymatic amenability of oak wood sawdust due to the porous morphology and cellulose crystallinity alterations after Organosolv treatment (methanol with an acid catalyst, at 160 °C and 2 h in autoclave). Ceaser et al. (2023) achieved pre-treatment optimisation using a DES (ChCl: Lactic acid at various molar ratios, at 80 °C and 2 h) combined with microwave heating, and investigated the chemical composition and crystalline structural changes of the milled softwood mixture. However, due to the many variables that need to be controlled (i.e. time, temperature, heating mechanism (conventional heating or microwave heating), biomass type, solvent type, biomass to solvent ratio, stirring speed etc.), results from different publications are not directly comparable. Additionally, insufficient knowledge of the energy consumption and thus techno-economic impact of different pre-treatment methods poses a major obstacle in process intensification and scale-ups.

To address the abovementioned knowledge gap, the aim of the present study is to investigate how different pre-treatment methods (i.e. alkali, Organosolv and DES process) influence the biomass fractionation and particularly the physiochemical changes of wood, with a view to informing process selection and product susceptibility for further chemical, thermal and biological upgrading. Regarding the material selection in this work, we studied two representative LCBs: a hardwood (oak) and a softwood (pine), so that the difference due to the nature and original chemical composition of LCB may be elucidated. The specific objectives are:

1) To compare the efficiency of an alkali (2.5 M NaOH and 0.4 M Na_2S), an Organosolv (70 % ethanol in water with 1 % w/w H_2SO_4) and a DES (p-Toluenesulfonic acid: Choline Chloride: Glycerol in 2:1:1 molar ratio) process on biomass fractionation, cellulose modification and lignin recovery;
2) To compare the physiochemical changes of woods (cellulose-rich product) before and after different pre-treatments using complementary characterisations, including chemical compositions, functional groups, thermal degradation behaviours, crystallinity structure, surface morphology and macro- and nano-structures, with a view to informing product suitability for use in a range of different applications such as biofuel production and nanoparticles;
3) To compare the energy consumption of different pre-treatments and provide insights towards process intensification and scale-up.

2. Materials and methods

2.1. Materials

Oak and pine wood chips were provided by Kastamonu Entegre (Türkiye) as by-products/waste from their manufacturing operations. The wood chips were firstly washed with deionised (D.I.) water to remove all impurities and dried at 60 °C until constant weight to remove any moisture. The wood chips were then mechanically milled by a cutting mill (Retsch SM2000, Germany) and passed through a 4 mm size mesh. The milled woods were then sieved to collect the materials at the size between 1.70 – 3.35 mm.

Sodium hydroxide (NaOH), sodium sulfide (Na_2S), sulphuric acid (H_2SO_4, 95–98 %), choline chloride (ChCl), glycerol (Gly), p-toluenesulfonic acid (PTSA), anthrone, glacial acetic acid, acetyl bromide, hydroxylamine hydrochloride, D-(+)-glucose, and cellulose standard (medium fibers, ≥ 90 % w/w of dry basis) were purchased from Merck, UK. Ethanol (absolute) was purchased from Scientific Laboratory

Supplies, UK. D.I. water was made by Milli-Q Plus water purification system (Merck KGaA, Germany).

2.2. Pre-treatment methods comparing three solvents

Three pre-treatment methods using three solvents were applied to the wood chips, namely a). Alkali process; b). Organic solvent process and c). Deep eutectic solvent (DES) process. Fig. 1 shows a schematic of the delignification and downstream processes to obtain both the cellulose-rich fraction (CRF) and lignin-rich fraction (LRF). For all three pre-treatments, the wood biomass-to-solvent ratio was controlled at 5 % solid loading (1 g of biomass + 20 g of solvent). The same microwave-assisted extraction (MAE) condition was applied using a Monowave 200 microwave (Anton Parr, UK) at 2.45 GHz. The sample mixtures were heated to the set temperature of 120 °C and held at this temperature for the required length of time (15, 30, 60, 120 and 180 min). A maximum incident power of 200 W was applied. Stirrer speed was set at 600 rpm. After the hold time, compressed air was applied to cool the sample down to 70°C before the Monowave system could be opened and samples can be taken out for downstream processes. Different downstream processes were applied for the pre-treatments as described below.

2.2.1. Alkali process (2.5 M NaOH and 0.4 M Na_2S)

The alkali process used 2.5 M NaOH and 0.4 M Na_2S in water as the extraction solution, following the method in Sarıoğlu et al. (2025) with some modifications. After the microwave treatment, 20 mL water was added to aid the transfer of the treated mixture into a centrifuge tube. The solid treated biomass (namely, cellulose-rich fraction (CRF)) was recovered by centrifugation at 3900 rpm for 20 min. To achieve the precipitation of lignin, a few drops of concentrated H_2SO_4 were added into the liquid supernatant until the solution reached approximately pH 5 and stored in a 4 °C fridge overnight. The lignin-rich fraction (LRF) was then separated by centrifugation at 3900 rpm for 1 h. Both the CRF and LRF were dialysed (cellulose membrane tubes, typical molecular weight cut-off=14,000 Da, Merck, UK) against D.I. water for 5 days to remove the salts or chemicals from the solvents. The CRF and LRF were then freeze-dried using a LyoDry freeze dryer (Mechatech Systems, UK) for yield calculations and further analytical characterisations. All experiments were performed in triplicates.

2.2.2. Organosolv process (70 % Ethanol with 1 % H_2SO_4)

For the organic solvent extraction, 70 % ethanol in water was used as the extraction solvent with 1 % w/w H_2SO_4 as the catalyst, following the method in Liu et al. (2020) with modifications. The same solid-to-liquid ratio, extraction temperature, time, microwave power, reaction vessel, and string speed were used as in the alkali process extraction. However, the downstream processes and lignin precipitation in the organic solvent were different. 20 mL ethanol was added to aid the transfer of the organic-solvent-treated mixture into a centrifuge tube. CRF was recovered by centrifugation at 3900 rpm for 20 min. An equal 20 mL volume of D.I. water was added to the supernatant and stored in a 4 °C fridge overnight. LRF was precipitated out and separated by centrifugation at 3900 rpm for 1 h. Then the same dialysis and freeze-drying steps applied

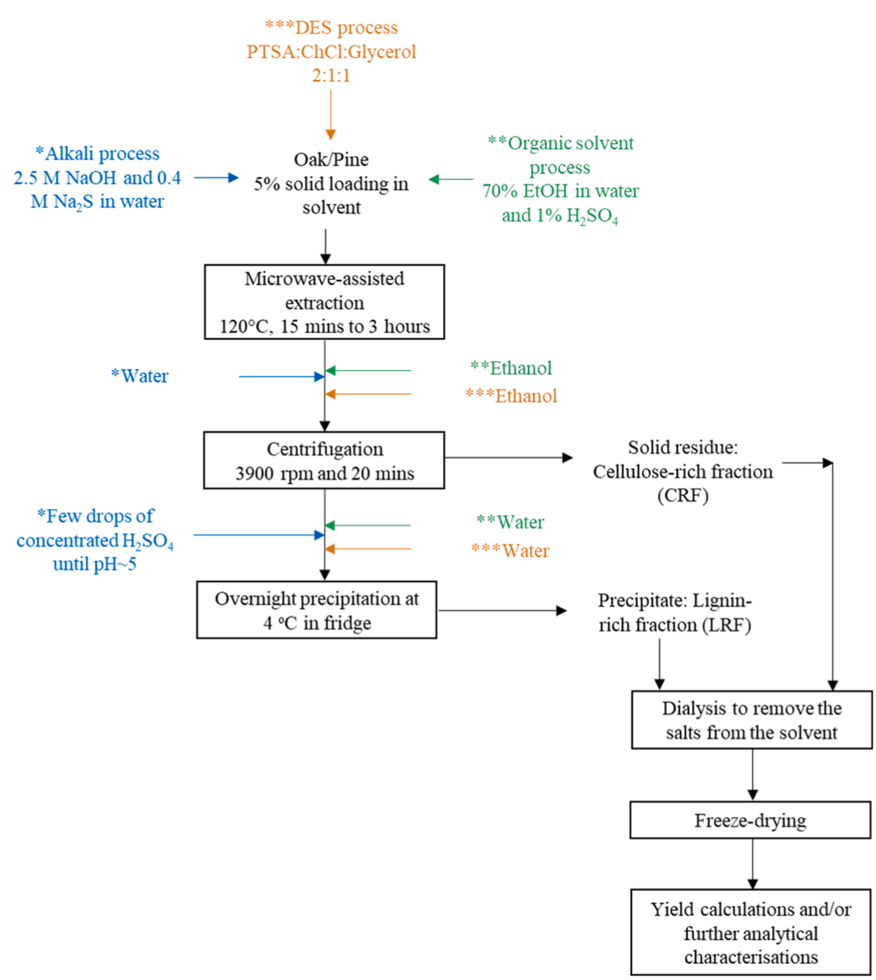

Fig. 1. Schematic of wood pre-treatment using microwave-assisted extraction with downstream processes for lignin recovery comparing the use of alkali solvent (*), organic solvent (**) and deep eutectic solvent (***).

to the organic-solvent-extracted CRF and LRF.

2.2.3. Deep Eutectic Solvent process (PTSA: ChCl: Glycerol in 2:1:1 molar ratio)

The DES process follows the method in Mao et al. (2023a). DES was synthesised by heating the mixture of PTSA, ChCl and Glycerol in a 2:1:1 molar ratio at 50 °C using a water bath, 30 min and constant stirring at 600 rpm, until a transparent and homogeneous solvent was formed. The DES process also followed the same microwave treatment as in the alkali and Organosolv process. The downstream processing for DES-extracted lignin recovery followed the same anti-solvent precipitation steps as described in the Organosolv process.

2.2.4. Product yield calculation

The percentage of biomass weight loss was obtained by the weight difference of wood (at dry basis) before and after the pre-treatment processes, as shown in Eq. (1):

$$\%Wood\ Weight\ Loss = \frac{Dry\ weight\ of\ raw\ wood(g) - Dry\ weight\ of\ CRF(g)}{Dry\ weight\ of\ raw\ wood(g)} \times 100\% \tag{1}$$

The yield of LRF was presented as the percentage content of LRF of dry basis per gram of raw wood, see Eq. (2):

$$\%Yield\ of\ LRF = \frac{Dry\ weight\ of\ LRF(g)}{Dry\ weight\ of\ raw\ wood(g)} \times 100\% \tag{2}$$

2.3. Product characterisations

2.3.1. Chemical composition

The changes of the main chemical components (i.e. cellulose and lignin) in the untreated wood and their resulting products (CRF and LRF) were characterised to compare the delignification efficiency of the three different solvents. Chemical composition characterisations were as follows.

2.3.1.1. Cellulose content characterisation by Bailey's method. The procedures for cellulose content measurement were developed from Bailey (1958) with modifications. Firstly, to allow the complete breakdown of cellulose contents in the biomass (for both untreated wood and CRF) into glucose monosaccharides, 100 mg of biomass were hydrolysed with 1 mL of 70 % v/v H_2SO_4 and incubated at 35 °C for 1 h in a water bath. Then the solution was added 11 mL of D.I. water (to achieve an acidic concentration ~ 1 M) and further incubated at 95 °C for 1 h. The mixture was cooled down immediately in ice and left to settle for 30 min. The supernatant from the mixture was collected and passed through 0.45 μm syringe filters (Scientific Laboratory Supplies, UK), then further diluted with D.I. water to appropriate concentrations if required. 1 mL of the above samples was mixed with 10 mL of 0.5 mg/mL anthrone in 70 % v/v H_2SO_4, then heated in a 95 °C water-bath for 10 min. After heating, the reaction was terminated by cooling immediately in ice. The mixtures were stored in the dark for 30 min for colour development before measuring with an UV-Vis spectrophotometer (Cary 60, Agilent Technologies, USA) at the wavelength of 625 nm. The standardisation curve was obtained using glucose solutions in a concentration range of 0–0.2 mg/mL (standardisation curve is reported in the supplementary material). The blank reference was made of 1 mL D.I. water in 10 mL anthrone reagent and used in UV-Vis measurements to eliminate the colour effect due to the anthrone. To calculate the cellulose content from the content of the hydrolysed glucose, a coefficient of 0.9 was applied. The imperial chemical equation of cellulose hydrolysis reaction is:

$$nC_6H_{12}O_6 \rightarrow (C_5H_{10}O_5)_n + nH_2O$$

Where, $C_6H_{12}O_6$ is glucose with molecular weight of 180 g/mol; and $(C_5H_{10}O_5)_n$ is the imperial formula for cellulose, and each cellulose block $(C_5H_{10}O_5)$ has a molecular weight of 162 g/mol.

Therefore, the cellulose content was presented as:

$$\%Cellulose\ content = \frac{0.9 \times Glucose\ concentration\left(\frac{mg}{mL}\right) in\ anthrone\ regent \times Total\ volume\ of\ solution\ added(mL)}{Dry\ weight\ of\ biomass(g)} \tag{3}$$

2.3.1.2. Lignin content characterisation by Acetyl Bromide Soluble Lignin (ABSL) Assay. The procedures of biomass digestion (for untreated wood, CRF and LRF) in acetyl bromide in glacial acetic acid followed the method in Barnes and Anderson (2017) and the aliquot was measured with a UV-Vis spectrophotometer (Cary 60, Agilent Technologies, USA) at the wavelength of 280 nm. The lignin standard solution was made using commercial Kraft lignin (KL) in a concentration range of 0–0.1 mg/mL (standardisation curve is reported in the supplementary material). Glacial acetic acid was used as the blank reference in UV-Vis measurements. The lignin content was presented as:

$$\%Lignin\ content = \frac{Lignin\ concentration\left(\frac{mg}{mL}\right) in\ ABSL\ solution \times Total\ volume\ of\ solution\ added(mL)}{Dry\ weight\ of\ biomass(g)} \tag{4}$$

2.3.2. FTIR analysis

The functional groups in both untreated wood and CRF were analysed and compared to the cellulose standard. LRF were analysed and compared to the lignin standard. An Attenuated Total Reflectance Fourier Transform Infrared (ATR-FTIR) spectroscopy (Cary 630, Agilent Technologies, USA) was used. The assignments of functional groups in the FTIR spectrum are referenced from Lu et al. (2017) and Sathawong et al. (2018). The spectra were taken in the wavenumber range between 4000 and 650 cm^{-1} with a resolution of 4 cm^{-1}.

2.3.3. TGA analysis

Thermo-Gravimetric analysis (TGA) (TA Instrument Q500, USA) was used to characterise the thermal degradation properties of the untreated wood and CRF, following the method Dewi et al. (2024) with modifications. Approximately 27 mg extracts were loaded on platinum pans. Extract samples were firstly heated at 10 °C/min under a Nitrogen gas at 100 mL/min from room temperature to 110 °C and held for 30 min to remove the moisture contents. Following this process, the temperature was firstly ramped at 5 °C/min to 500 °C, then 10 °C/min to 900 °C. The samples were isothermal at 900 °C for 10 min to obtain the volatile matter content. This temperature was held for 7 min, before switching to air at 100 mL/min for 10 min to ensure complete combustion for fixed carbon and ash content. The data were processed using TA Universal Analysis 2000 Software 4.5 A. The derivative weight loss (% wt/°C) versus temperature was recorded.

2.3.4. XRD analysis

X-Ray Diffraction (XRD) analysis was used to characterise the

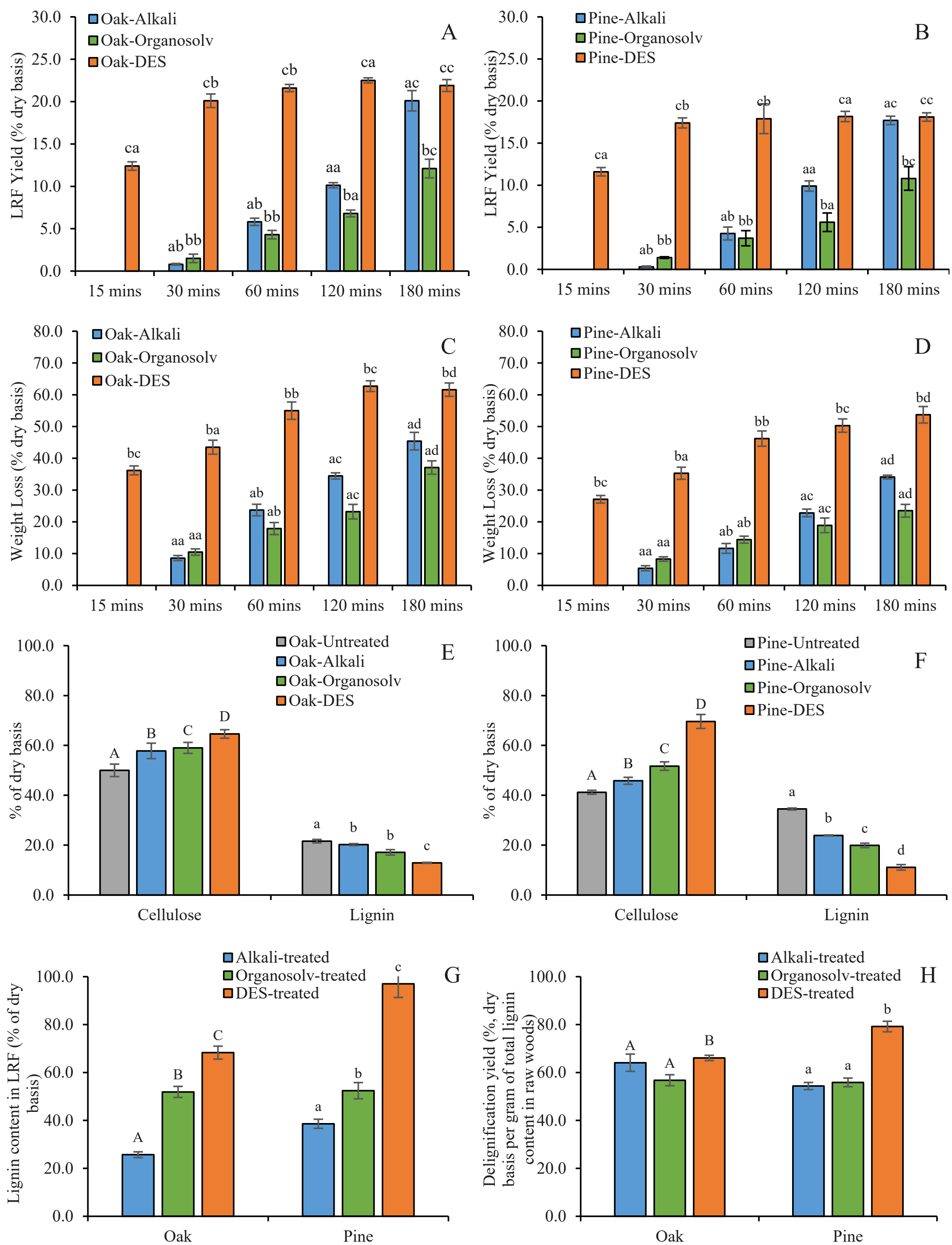

Fig. 2. Comparison of the delignification performance between alkali, Organosolv and DES process of oak and pine wood. (A-B). LRF yield. (C-D). Wood weight loss. (E-F). Wood compositional changes. (G). Lignin content in LRF determined by ABSL assay. (H). Delignification efficiency as % content of dry basis per gram total lignin content in raw woods. Different letters in the same data figure indicate the significant difference ($p < 0.05$).

crystallographic structure of the untreated wood and CRF. The analysis was performed by a D2 Phaser X-ray diffractometer (Bruker, USA) with a Cu Kα source. The diffraction patterns were obtained at Bragg's angles (2θ) varying from 5 to 50° at the rate of 4°/min. Two typical peaks corresponding to the (002) and (101) lattice planes of cellulose I type were respectively shown at Bragg's angles (2θ) of 22.3° and 16.1°, reflecting the crystalline structure (Yu et al., 2022). The degree of crystallinity was calculated using the Bruker Diffrac Eva Software V4.1.

2.3.5. SEM analysis

The morphology of the untreated wood and CRF were examined by an Ultra Plus Field Emission Scanning Electron Microscopes (FE-SEM, Zeiss, Germany) operated at 3 kV. The samples were sputter-coated with gold for 25 s prior to the measurement.

2.3.6. SAXS analysis

To characterise the nanostructure of the untreated wood and the resulting CRF after pre-treatments, small-angle X-ray scattering (SAXSPoint 5.0, Anton Paar, UK) was used at a sample-to-detector distance of 500 mm, which resulted in a wavevector (q) range between ≈ 0.1 nm^{-1} and ≈ 6.9 nm^{-1}. Samples were placed on a heated-cool multi-sample holder and preconditioned by isothermally waiting at 90 °C for 5 min under vacuum. The samples were then cooled down to 40 °C for measurements. The samples were placed in a way that the microfibers are oriented vertically. The SAXS data for each sample was collected for 15 min with five frames with 180 s collection time. The transmission and background (an empty cell) were also measured for each sample for proper data reduction and subtraction. SASView Software was used for data processing.

2.4. Statistical analysis

To understand the influence of different pre-treatment methods, controlled single-factor experiments were performed by changing only one variable at a time (pre-treatment solvents, extraction time and biomass types) while carefully controlling all the other independent factors (e.g. temperature, microwave power, solid loading, sample volume etc.). The product yield (wood weight loss % and LRF yield %) with error bars were calculated based on triplications, and the resulting CRF and LRF products from the triplicated pre-treatments were combined to exclude the difference of each extraction in further analytical characterisations. The results and error bars from chemical composition and crystallinity index were determined by triplications on the combined products. All data were expressed as mean values ± standard deviation (SD) ($n = 3$). Statistical analysis of data was performed using SPSS Statistics (IBM SPSS Statistics, Version 29.0., USA). Data were subjected to a one-way ANOVA with the Duncan test and the probability value of $p < 0.05$ was considered significant.

3. Results and discussion

3.1. Influence of pre-treatment solvents on biomass delignification

3.1.1. Product yield

To obtain an understanding of the delignification performance of traditional and novel pre-treatment methods, systematic comparisons between an alkali (2.5 M NaOH and 0.4 M Na_2S), an Organosolv (70 % ethanol with 1 % w/w H_2SO_4) and a DES (PTSA: ChCl: Glycerol in 2:1:1 molar ratio) were performed on both oak and pine wood. The pre-treatment was microwave-assisted at 120 °C according to the process optimisation from our previous work (Mao et al., 2023a), and extraction times from 15 min to 180 min were studied. Results present both the lignin-rich fraction (LRF) yield (% dry wood), which determined the effectiveness of lignin recovery, and the wood weight loss (% dry wood) before and after the pre-treatments, which corresponded to the preservation of the cellulose-rich fraction (CRF).

For both oak and pine wood, the DES process exhibits enhanced ability in delignification compared with alkali and Organosolv processes. For oak wood, DES yields 20.1 % of LRF in only 30 min of extraction time, while alkali process requires 180 min to obtain a similar LRF yield of 20.1 % and the Organosolv process only achieves its highest LRF yield of 12.1 % at 180 min (Fig. 2A, $p < 0.05$). Similar results are found for pine wood that DES obtains LRF yield of 17.4 % at 30 min, while alkali and Organosolv achieve their highest LRF yield of 17.7 % and 10.8 % respectively both at 180 min (Fig. 2B, $p < 0.05$). Similar results have been reported in the literature, where a temperature of 160–200 °C and more than 2 hrs are often required to obtain a lignin yield above 60 % of the total lignin content in the studied biomass when alkali or organic solvents are used (Chio et al., 2019; Nitsos et al., 2016; Parot et al., 2022), while DES can achieve similar lignin recovery in only 30–60 min (Kohli et al., 2020; Mao et al., 2023a). Although the DES process at a longer treatment time slightly increases the LRF yields, taking into account the cycle time and thus energy consumption compared with the negligible yield increase, 30 min time is considered the best extraction time of DES process for both oak and pine wood. For alkali and Organosolv processes, further processing time longer than 180 min is not included as this is time used in most literatures in laboratory set-ups (Parot et al., 2022; Rahman et al., 2024) and commonly reported in the industrial process (Chio et al., 2019; Pola et al., 2022; Woiciechowski et al., 2020). All product characterisations discussed in the below sections were obtained at the abovementioned conditions.

Comparing the response of oak and pine wood under different treatments, pine wood has lower LRF yield than oak wood regardless of the solvent used. This is contrast to the fact that raw pine wood (softwood) had a higher lignin content of 34.5 % compared to that of raw oak wood (hardwood) of 21.6 % (characterised by ABSL method, Figs. 2E and 2F). Similar results were reported by Nitsos et al. (2016), where birch wood (hardwood) had higher wood weight loss than spruce wood (softwood) under both alkali treatments using 10–20 % NaOH solution (similar alkalinity as the alkali solvent in this study) and 60 % ethanol solution with 1 % H_2SO_4. This might be because softwood generally has a more recalcitrant chemical structure, as well as lignin and hemicellulose arrangement, causing it to be more difficult to delignify compared with hardwood (Sirviö et al., 2023). However, when using other DES systems such as choline chloride - lactic acid and choline chloride - levulinic acid, Alvarez-Vasco et al. (2016) reported higher lignin recovery from Douglas fir wood (softwood) than poplar wood (hardwood) at all tested temperatures ranging from 90 to 180 °C, showing the potential of DES in overcoming the structural recalcitrance of softwood and achieving higher delignification. The reason why this is not observed in this present work may be attributed to the structural difference of lignin in soft and hardwood. The syringyl units (S), which are present in the hardwood lignin but absent from the softwood are substituted by two methoxy groups that limit condensation reactions at the ortho positions on the aromatic ring (Liu et al., 2020). Therefore, lignin condensation during the pre-treatment is potentially more pronounced in the pine than oak causing negative impact on the lignin recovery. This implicates the importance of solvent selection in LCB processing and a fundamental understanding in interactive mechanisms between different DES systems and biomasses; this is not within the scope of this work and future work should elucidate this.

The changes in wood weight after the pre-treatment correlated with the LRF yield. Between different pre-treatments, it exhibits almost a similar amount of wood weight removal to obtain a comparative LRF yield (Figs. 2C and 2D). For example, DES pre-treatment at 30 min achieves 20.1 % of LRF yield required 43.5 % biomass weight loss from oak, while similar LRF yield of 20.1 % and weight loss of 45.4 % are found by alkali process at 180 min ($p < 0.05$). Similarly, to obtain 12.1 % oak LRF yield Organosolv process at 180 min loses 37.1 % of wood weight, while results from the DES process at 15 min are 12.4 % and 20.2 % respectively ($p < 0.05$). Although the exact mechanism of lignin cleavage in DES remains elusive, and the physico-chemical properties of lignin originated from various biorefinery processes is still very variable, it is generally believed the key step of lignin extraction is the cleavage of the intermolecular C-O linkages existing between lignin-carbohydrate complexes (LCC), particularly the α-O-4 and β-O-4 bonding (Liao et al., 2020). The work presented here indicates the requirement of a certain degree of structural breakdown to release the lignin, which shows independence to the types of pre-treatments. It is worth noting that the weight loss value is much higher than the amount of LRF collected, suggesting a proportion of unrecovered components lost in the extracting solvents. The content of this proportion varies from 7.8 % to 40.2 % in oak wood delignification and 5.1–35.6 % in pine wood delignification. This loss is most likely to be predominantly hemicellulose and some lower molecular weight lignin, which can dissolve in the pre-treatment solution but are unable to precipitate due to their smaller molecular weight and/or are lost during the dialysis process (Zhang et al., 2022). Hemicellulose is an important fraction of LCB (accounting for 20–30 % of the biomass dry weight (Wang and Lee, 2021)) and can dissolve in the pre-treatment solution but is unable to precipitate due to its smaller molecular weight than lignin (Zhang et al., 2022). This suggests the importance of adding in a hemicellulose recovery step in the downstream process, which only very little research has investigated to date and further work is required.

3.1.2. CRF composition and wood compositional changes

The cellulose, hemicellulose and lignin contents in the raw wood and respective CRFs were determined to capture the compositional changes of wood before and after different pre-treatments. CRFs determined were obtained from their highest delignification condition tested: alkali process (180 min), Organosolv process (180 min), DES process (30 min), all at 120 °C (detailed discussion in Section 3.1.1). Results were presented in Figs. 2E and 2F. The untreated oak wood contains 50.0 % cellulose, 21.6 % lignin, and 28.4 % hemicellulose, while the untreated pine wood contains 41.2 % cellulose, 34.5 % lignin, and 24.3 % hemicellulose; those results are within the compositional ranges of hardwood and softwood reported in the literature (Kumar and Sharma, 2017). Both oak and pine wood have increased cellulose compositions and reduced lignin compositions after the pre-treatments, among which the DES process exhibits a higher degree of wood compositional alterations. To better illustrate the delignification yield comparing the three pre-treatments, Fig. 2H plots the delignification efficiency as % lignin extracted on a dry basis per gram total lignin content in raw wood, where DES again shows the highest ability to remove 66.1 % and 79.2 % of the total lignin contents of the studied oak and pine materials respectively ($p < 0.05$). In comparison, our previous work (Mao et al., 2023a) using the same DES solvent has shown almost complete lignin removal of 95.5 % from cocoa bean shells at 130 °C, 30 min. This work suggests higher structural recalcitrance of woody biomasses than cocoa bean shells, and future work should elucidate the process optimisations based on different biomass selections.

3.1.3. LRF composition

The content of lignin in LRF precipitates was characterised by ABSL assay and illustrated in Fig. 2G. Corresponding to the reduced lignin content in CRF, the LRF from DES process had highest lignin content, followed by Organosolv and finally alkali process, suggesting solvent selectivity targeting lignin extraction. DES process was particularly promising for pine wood recovering almost pure lignin (97.0 % lignin content in its LRF) compared than oak wood (68.3 %) ($p < 0.05$). The unqie effectiveness of DES process on softwood was also reported Alvarez-Vasco et al. (2016), where LRF precipitate from Douglas fir (soft) wood presented a much higher lignin content of 88.4 % than that of 66.2 % from Poplar (hard) wood. The lignin contents in Organosolv-recovered LRF were 51.9 % from oak and 52.4 % from pine ($p < 0.05$), which were relatively lower than those reported in the literature. Liu et al. (2020) recovered pine LRF with 91 % lignin content and oak LRF with 86 % lignin content using 65 % ethanol-water solution, although in their work the extraction was conducted at a much higher temperature of 165–180 °C. In addition, LRF from alkali process had the lowest lignin content from both oak (25.7 %) and pine (38.6 %) ($p < 0.05$). Results were not surprising as the alkali (Kraft) process was designed based on the 'cellulose-first' approach, in which although it offered comparable delignification from the wood, the recovery of the lignin was not optimised (Haq et al., 2020). The structural difference between alkali-, oragnosolv-, and DES-recovered LRF were further discussed in Section 3.2.1.

3.2. Influence of pre-treatment solvents on biomass physicochemical changes

CRFs were obtained as the solid fraction after pre-treatment and their chemical compositions were discussed in previous Section 3.1.2. To further understand the influence of alkali, Organosolv and DES processes on the physiochemical changes of wood, CRF products were characterised by their chemical functional groups (FTIR), thermal degradation properties and pyrolysis behaviour (TGA), degree of crystallinity (XRD), surface morphology (SEM) and nanostructure (SAXS). It was hoped these complementary characterisations could provide insights informing the product upgrading routes for value-added applications.

3.2.1. Chemical functional groups

To investigate the functional groups and chemical compositional changes of wood during the pre-treatments, FTIR spectra in the 3600–850 cm^{-1} wavenumber range were studied and compared with the cellulose standard and untreated wood from both CRF (Figs. 3A and 3B) and their respective recovered LRF (Figs. 3C and 3D).

Generally speaking, both CRFs and their respective untreated wood show similar trends of peaks as cellulose standard because of the presence of cellulose as the predominant component in wood, although some peaks were more intense than others comparing different pre-treatments and wood sources, and the results are discussed below (Figs. 3A and 3B). Firstly, the FTIR characterisations support the chemical composition results and corresponded to the higher delignification efficiency results of DES compared with alkali and Organosolv processes (previously mentioned in Section 3.1). The spectra of DES-treated CRF present higher similarity to cellulose standards with higher peak intensity than the spectra of alkali- or Organosolv-treated CRF, while untreated wood has the lowest peak intensity. Specifically, at 1031 cm^{-1} wavenumber which is attributed to the C-O stretching primarily from cellulose structure, DES-treated CRF exhibits the highest peak absorbance followed by CRFs from Organosolv and finally alkali process. This corresponds to the higher cellulose content from DES-treated CRF comparing the other two pre-treatments as reported previously (Figs. 2E and 2F), supporting the promoted delignification ability of DES over the other two processes. Another peak at wavenumber 1507 cm^{-1} representing the C-O stretching in the aromatic ring structure from lignin was most obviously shown in the alkali- and Organosolv-treated CRF as well as the untreated woods indicating the presence of lignin but absent from cellulose standard. In the meantime, DES-extracted CRF from oak and pine shown opposite response, indicating the DES's ability in complete removal of aromatic lignin from the pine but ineffectiveness for oak. Those aromatic lignin components were later recovered in their respective LRF and showing higher transmittance of this peak in pine LRF than oak LRF (Figs. 3C and 3D), results were further discussed later in this section. Secondly, the cellulose structure is found better preserved in DES pre-treatment and thus may exhibit better potential for value-added applications. The peak at the wavenumber ranging 3400–3200 cm^{-1} is primarily attributed to the phenolic -OH groups in cellulose (although the –OH groups (phenolic and aliphatic) from the hemicellulose and lignin content remained in the CRF are also shown in this region, their contents are less than the cellulose content as previously mentioned in Figs. 2E and 2F). The intensity of these –OH

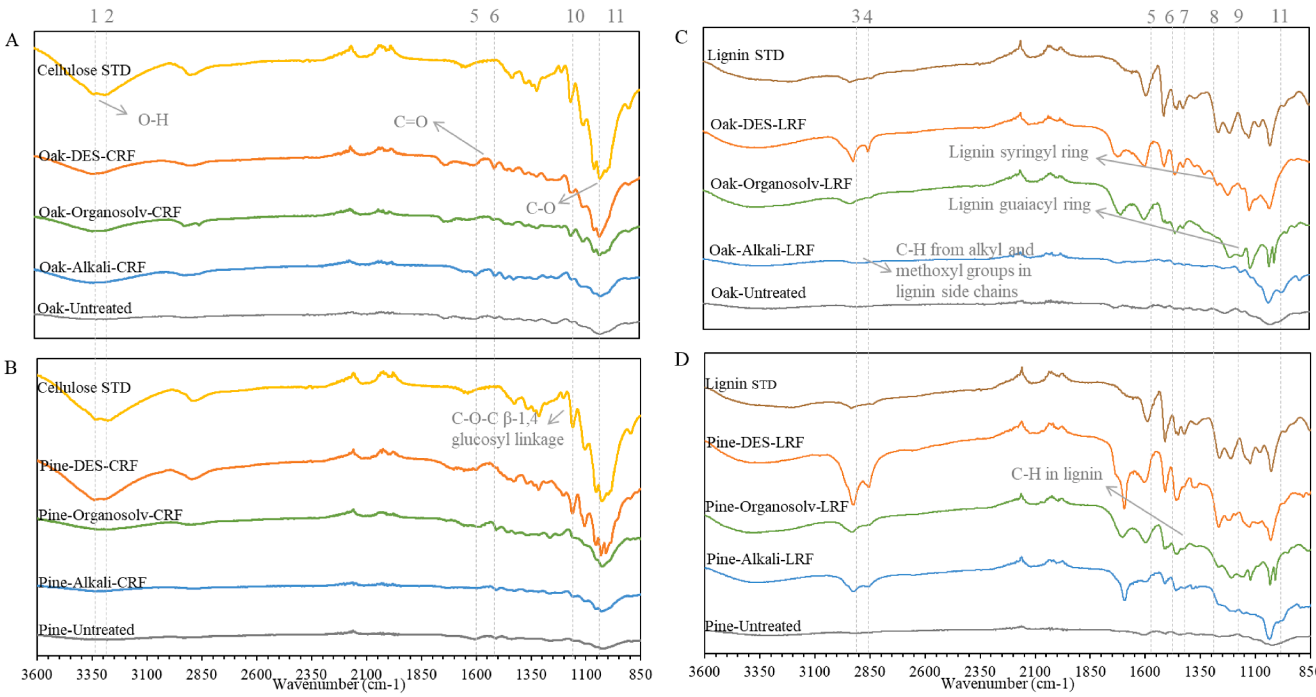

Peak label	Wavenumber (cm^{-1})	Vibrating type	Functional groups
1, 2	3400-3200	O-H	-OH of alcohols, phenols and acids
3, 4	2923-2852	C-H	C-H stretching in alkyl chains adjacent to an aromatic lignin and CH variation in lignin methoxyl groups
5, 6	1600-1507	C=O	Conjugated p-substituent carbonyl and carboxyl & aromatic ring in lignin
7	1454	C-H	C-H deformation in lignin
8	1325	C-O	Syringyl ring from lignin S sub-units
9	1208	C-O	Guaiacyl ring from lignin G sub-units
10	1156	C-O-C	C-O-C β-1,4 glucosyl linkage of cellulose
11	1031	C-O	C-O in primary aliphatic OH groups and ether structures

Fig. 3. FTIR spectra of cellulose standard and CRF product by alkali, Organosolv and DES pre-treatments, and their assignments of signals to functional groups. (A-B). FTIR of CRF products from oak and pine compared with cellulose standard and respective untreated wood; (C-D). FTIR of LRF products from oak and pine compared with lignin standard and respective untreated wood. The assignments of functional groups in the FTIR spectrum are referenced from Lu et al. (2017) and Sathawong et al. (2018).

structures maintain similar high content in DES-extracted CRF compared with the cellulose standard but is much less in alkali- and Organosolv-treated CRFs. The phenolic contents in the LCB could potentially enhance its susceptibility to enzymatic hydrolysis resulting in higher bioethanol production rate (Stamogiannou et al., 2021). Additional evidence shows DES-treated CRFs from both oak and pine wood exhibit highest peak absorbance at 1156 cm^{-1}, which presents the β-1,4 glucosyl linkage in cellulose, while this peak is least intensive from alkali-treated CRF.

Spectra from LRF showed much higher resemblance to the lignin standard than the untreated wood, informing their lignin-rich nature (Figs. 3C and 3D). Specifically, peak intensity at wavenumber 1454 cm^{-1} that attributing to the C-H deformation in lignin structure was in agreement with the lignin contents results in LRF (previously shown in Fig. 2G), where DES-recovered LRF with higher lignin content presented higher peak absorbance, followed by oragnosolv-recovered LRF and finally alkali-recovered LRF. This peak was particularly obvious in the pine LRF recovered by DES showing almost similar peak intensity as the lignin standard, as the lignin content in this LRF reached 97 % as pure as the standard (Fig. 2G). Results also evidented the structure difference between the LRF recovered by different pre-treatment, with DES-recovered LRF presenting several peaks at certain wavenumbers specifying its unique and interesting structures, which were less obvious or absent in the LRF obtained by alkali and Organosolv process in the present study. Firstly, absorbance at 2923 cm^{-1} and 2852 cm^{-1} were attributed to C-H stretching in alkyl chains adjacent to an aromatic centre, and CH variation in methoxyl groups respectively in the lignin side chains. These peaks were much higher for the DES-recovered LRF implying a greater degree of methylation than Organosolv-recovered LRF, while partial to almost complete degradation of methoxyls from the lignin aromatic ring occurred in alkali process. Comparing different wood sources, pine wood after pre-treatment had better preserved methylation than oak wood. The peak at 1600–1507 cm^{-1} represented the aromatic skeletal stretching in the aromatic ring structure in lignin, and it was more evident from DES-extracted LRF but negligible from alkali-recovered oak LRF. The lower content of aromatic rings as well as lower degree of methylation (leading to more free -OH phenolic groups) made alkali and Organosolv lignin more hydrophilic than DES lignin (Liao et al., 2020). Furthermore, LRF from different pre-treatments and wood sources presented different content of lignin sub-units, showing its syringyl (S) and guaiacyl (G) sub-units respectively at wavenumber 1325 cm^{-1} and 1208 cm^{-1}. The absence of S sub-unit in softwood (Liu et al., 2020) was confirmed by the disappearance of peak in pine CRF at 1325 cm^{-1}. DES process again exhibited better ability in preserving both the S and G sub-unit, while alkali was the most ineffective process. Although improved hydrophilicity and water solubility may increase its capability to be used in certain value-added applications, the aromatic rings, degree of methylation as well as the sub-units were also related to lignin functionality (Liao et al., 2020). For example, Sumerskii et al. (2017) has

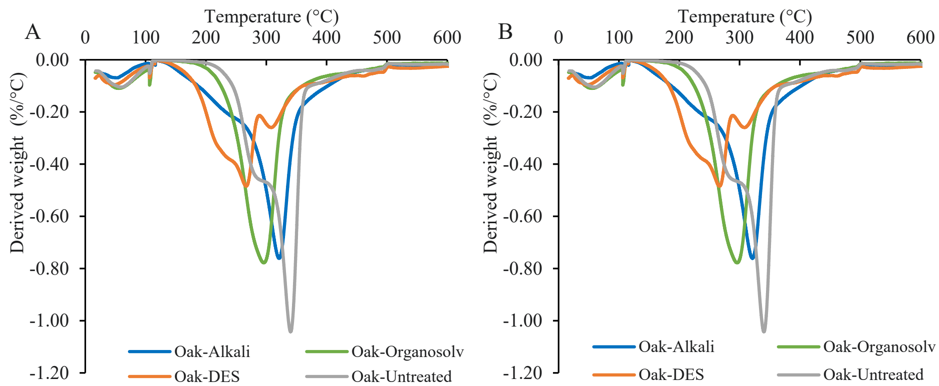

	Oak wood		Pine wood	
	T_{max} (°C)	R_{max} (%/°C)	T_{max} (°C)	R_{max} (%/°C)
Untreated	340	-1.04	346	-1.07
Alkali-treated	321	-0.76	326	-0.74
Organosolv-treated	295	-0.78	290	-0.69
DES-treated	267 (1st peak) 308 (2nd peak)	-0.48 (1st peak) -0.26 (2nd peak)	210 (1st peak) 313 (2nd peak)	-0.49 (1st peak) -0.45 (2nd peak)

Fig. 4. Derivative thermogravimetry (DTG) curves of wood before and after alkali, Organosolv and DES pre-treatments. (A). Oak wood. (B). Pine wood. T_{max}: temperature at the maximum weight-loss rate; R_{max}: maximum decomposition rate.

reported that lignin with a higher degree of methylation rendered better antioxidant and antimicrobial properties; while Maia et al. (2019) suggested the relevance of the contents of phenolic group attached to lignin's aromatic rings and its higher reactivity. Results in this study therefore offered insights in the process and material selection meeting product requirements for different applications of lignin.

3.2.2. *Thermal degradation behaviour*

TGA was performed to investigate the influence of alkali, Organosolv and DES pre-treatment on the thermal degradation of both oak and pine wood. The derivative thermogravimetry (DTG) curves (Fig. 4) illustrate two stages of thermal degradation. In the first stage where the temperature is increased from room temperature to 110 °C, there is a small amount of biomass weight loss mainly due to the moisture evaporation and the difference is insignificant between the untreated woods and different CRFs. As a control measure in this study, both raw wood chips and resulting CRFs were dried before TGA analysis so that the moisture contents were minimized (the raw oak and pine wood chips were oven-dried at 60 °C until constant weight while the CRFs were freeze-dried). Given that high moisture content often leads to reduced heat content, increased heat loss due to evaporation and superheating of vapour and risks of spontaneous ignition or combustion (Mierzwa-Hersztek et al., 2019), reducing the moisture content (i.e. drying) plays an important role in biomass pyrolysis. The majority of the thermal degradation of wood occurs at the second stage during a temperature range of 110 – 500 °C. All CRFs present peak shifts in DTG curves to lower temperatures compared with the untreated wood. Additionally, other than Organosolv- or alkali-treated CRF, which only presents a single distinguished peak similar to the untreated woods, DES-treated CRF shows completely different profiles of DTG. In the case of DES-treated CRF from oak, a peak is observed at a maximum temperature of 267 °C with a shoulder at the side at approximately 225 °C; besides, a minor peak at 308 °C is also detected. DES-treated CRF from pine also presents two peaks: the first one of which appears at a lower temperature of 210 °C and without the shoulder than oak CRF, and the other one at a similar temperature of 313 °C. The thermal degradation of the LCB involves the three major types of polymers, among which hemicellulose devolatilises first at low temperatures ranging from 200 to 250 °C, cellulose decomposes at higher temperatures ranging between 300 and 400 °C, whereas lignin requires wider temperature ranges for complete degradation, up to 900 °C (Bensidhom et al., 2018; Yang et al., 2007). These results suggest effective biomass fractionation by DES pre-treatment through the removal of lignin (DTG profiles shifted to lower temperatures, results corresponded with DES's delignification performance discussed previously in Section 3.1) and the separation of

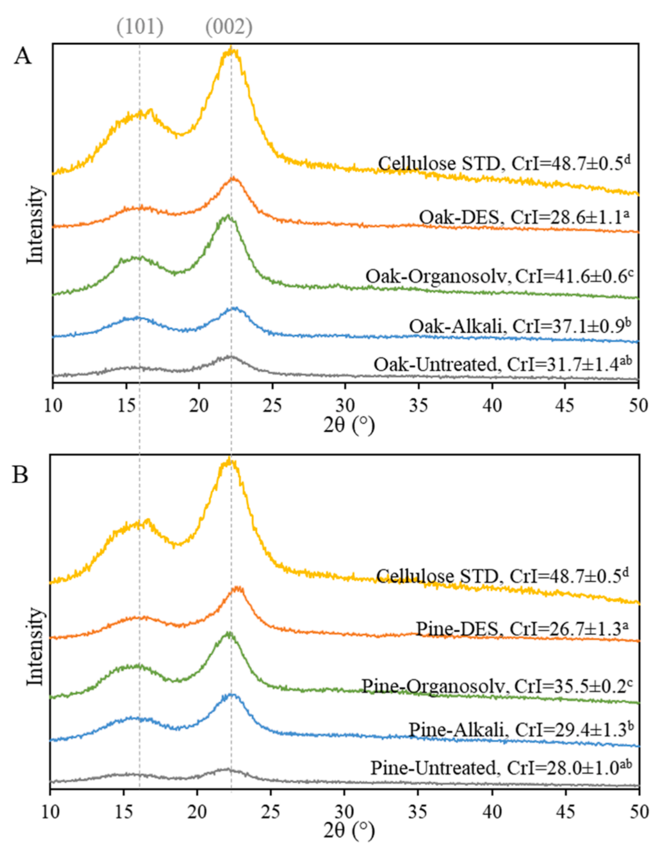

Fig. 5. X-Ray Diffraction (XRD) spectra and calculated crystallinity index (CrI, %) before and after alkali, Organosolv and DES pre-treatments. (A). Oak wood. (B). Pine wood. Different letters in the same data figure indicate the significant difference ($p < 0.05$).

hemicellulose (first peak) and cellulose structure (second peak).

The thermal degradation behaviour is an important characteristic informing the potential of woods for sustainable energy through various thermochemical conversion routes such as combustion, gasification and pyrolysis. Comparing the three pre-treatments, DES-treated CRF not only initiate its thermal degradation at lower temperature requirement (T_{max}), also exhibits significantly decreased decomposition rates (R_{max}). Literature has emphasised the importance of pre-treatment for the thermochemical conversion of LCB, as it decreases the degree of polymerisation and increases the internal surface area of the treated biomass (Ashokkumar et al., 2022). Additionally, the removal of lignin during the pre-treatment also enhances the bio-oil yield (Hoang et al., 2021). To conclude, results suggest DES pre-treatment could significantly improve the wood's susceptibility to thermal degradation and thus the best potential for pyrolysis applications compared to the other two pre-treatment methods.

3.2.3. *Crystalline structure*

X-Ray Diffraction (XRD) was performed to characterise the crystallinity structural changes of the wood after different pre-treatments. The full XRD spectra and the crystallinity index (CrI) of the wood samples determined by the ratio of the crystalline region (peak) to the amorphous region (valley) was presented in Fig. 5. In the untreated wood, oak presents higher crystallinity (showing CrI of 31.7 %) than pine (28.0 %), which is attributed to the higher cellulose and lower lignin contents in oak (wood composition results in Figs. 2E and 2F). Results show increased wood crystallinity for both oak and pine wood, which are particularly significant after the Organosolv process (showing CrI of 41.6 % for oak and 35.5 % for pine) and less obvious after the alkali process (showing CrI of 37.1 % for oak and 29.4 % for pine) ($p < 0.05$). This corresponds with the higher delignification ability of Organosolv than alkali process, as lignin is an amorphous component and hence the removal of lignin increased the wood's crystallinity. In contrast, DES pre-treatment causes decreased wood crystallinity (showing a CrI of 28.6 % for oak and 26.7 % for pine) ($p < 0.05$). Although DES-treated CRF has the highest delignification presenting the highest cellulose and lowest lignin contents compared to other CRFs, it indicates the transformation of crystalline cellulose into an amorphous state in this studied DES. This might be due to the higher dissolution of cellulose in DES that disrupted its crystalline structure, while cellulose is commonly recalcitrant in alkali or Organosolv solutions (Hattori and Arai, 2016).

The crystallinity is an important characteristic of cellulose components, determining its potential towards different functionality and applications. Firstly, it has been found that amorphous cellulose has less thermal stability and degrades at a relatively lower temperature compared with the crystalline cellulose, attributing to the absence of several intra- and inter-molecular H-bonds that are contained in crystalline cellulose and which preserves the sugar ring structure during pyrolysis (Chen et al., 2020). This corresponds with the TGA results presented in Section 3.2.2, that DES-treated CRF with less crystallinity showed thermal decomposition at lower temperatures, and thus exhibits better potential for applications such as combustion, gasification, and pyrolysis as energy sources. Secondly, reducing the crystalline degree of LCB prior to its bioconversion has been found to improve the material's enzymatic accessibility and hence enhance the bioethanol yield (Xu et al., 2019). The results presented here therefore indicate the potential effectiveness of DES pre-treatment in bioethanol production. However, other value-added applications target the crystalline derivatives of cellulose, such as microcrystalline cellulose (MCC) and nanocrystalline cellulose (NCC) (Debnath et al., 2021). Higher crystallinity is typically credited for higher modulus of elasticity, higher stiffness, and rigidity, contributing to higher mechanical properties (Sankhla et al., 2021). Crystalline cellulose is a suitable candidate as a load-bearing material or reinforcing agent in various food, chemical and pharmaceuticals fields, including bio-based composites, packaging, coating, and hydrogels (Tarhanlı and Senses, 2023). In those cases of applications, Organosolv pre-treatment exhibits the best potential.

3.2.4. *Macro- and nano-structure*

Scanning electron microscopy (SEM) was performed to observe the microscopic level structural change and morphology of the woods before and after treatment. The cross-sectional images of the raw and treated chips are presented in Fig. 6. The lumens of the wood could be observed for both oak and pine wood types; however, vessels are present only in the oak wood representing its hardwood characteristic. Regardless of the pre-treatment type, the wood structure changes significantly compared with the original dense and highly ordered structure of the native wood. When comparing the three different pre-treatments, the alkali process exhibits the best preservation of the wood structure, where the hierarchical microporous structure of wood is still visible even after 180 min-long treatment. However, the structural integrity of the woods is completely disrupted after DES process and only the scattered fibres can be observed. This is consistent with the results from chemical and gravimetric analysis (details seen Sections 3.2.1 and 3.2.2) as more lignin is separated from the woods by the DES compared with alkali and Organosolv methods, leading to wood structural breakdown. Additionally, the fibrillar cellulose structure loses its order and orientation due to the effective dissolution of the cell wall in DES (also seen Section 3.2.3). The SEM images also confirm the effectiveness of Organosolv pre-treatment to breakdown the wood recalcitrance as an intermediate between the alkali and DES pre-treatments.

SAXS, being a powerful non-invasive structural probe, provides

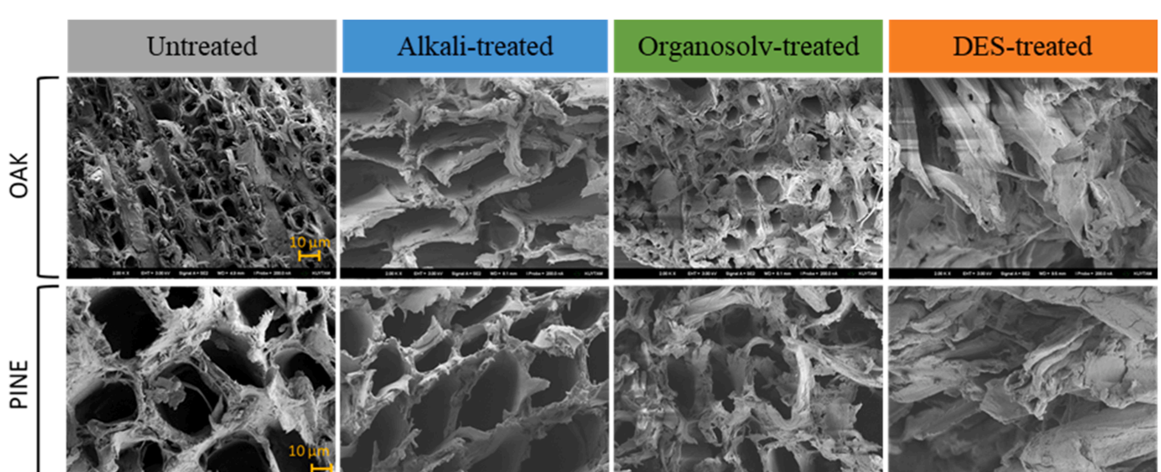

Fig. 6. Scanning Electron Microscopes (SEM) images of oak and pine wood before and after alkali, Organosolv and DES pre-treatments.

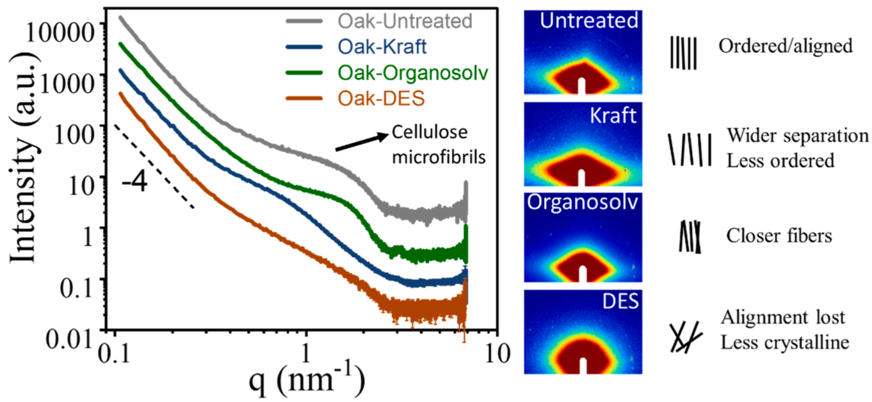

Fig. 7. Small-angle X-ray Scattering (SAXS) intensity profiles (shifted vertically for clarity of the comparison) for untreated and after different pre-treatments. The pictures are the raw detector data showing the level of ansiotropy of the scattering due to cellulose microfiber orientation.

further insights into process-dependent structural changes at the nanoscale. The SAXS intensity from wood is due to the hierarchical porous structure and the crystalline cellulose microfibrils forming bundles in the presence of amorphous lignin and hemicellulose. The removal of lignin (and/or hemicellulose) distorts the nanoscale distance between the single microfibrils as well as their orientation in the S2 layer of the cell wall (Penttilä et al., 2020). These structural changes can be captured in the SAXS data and complement the SEM results. The wavevector-dependent (isotropic) intensity profiles for the oak wood samples (trends were similar for the pine wood) are compared in Fig. 7 along with representative detector intensity data showing the changes in the anisotropic alignment of the cellulose fibrils upon treatment. Two dominant structural features are noticed in the I(q) data. In the low-q regime, typically q << 0.3 nm^{-1} (corresponding to length scales, 2π/q >> 20 nm), a strong intensity upturn is common for all samples and can be related to the lumens and/or large nano/micropores inherent to the wood structure. The $I \sim q^{-4}$ dependence is a characteristic of the sharp interface of the cellulose microfibril bundles with these micro/macro pores and it remains the same for all samples. Note that information about size changes of the large pores cannot be obtained as the SAXS length scale is not sufficiently large to observe the respective Guinier regions.

In the intermediate q (between 0.3 nm^{-1} and 3 nm^{-1}, corresponding to length scales from 2 nm to 20 nm), the form factor of the cellulose microfiber bundles dominates the intensity, giving rise to a hump in the intensity data. Upon Organosolv pre-treatment, the location of the peak position observed at q ≈ 1.8 nm^{-1} (a length-scale of 3.5 nm) for the raw wood shifts slightly to higher q and becomes narrower, suggesting a decrease in the distance between the cellulose microfibers without significantly altering the microstructure of the bundles. This causes a compaction of the cell wall seen in the SEM images. A similar trend was previously observed upon drying of wood samples leading to a decrease of distance between microfibrils; hereby the effect is caused by the removal of lignin and/or hemicellulose binders in the bundles. The alkali pre-treatment, on the other hand, makes the profile very broad and shifts to lower q values, with a maximum at q ≈ 0.8 nm^{-1} (corresponding to a length-scale of ≈ 8 nm), suggesting a swelling of the cell wall by increased separation of microfibril bundles. This contrasts with the Organosolv pre-treatment likely due to the insolubility of cellulose in ethanol causing a shrinkage. Nevertheless, the DES treatment shows the least distinctive and broad feature of cellulose microfibrils, suggesting the loss of order in microfibril bundles and/or the crystallinity of the individual cellulose fibers. The XRD results (Section 3.2.3) showed less crystalline CRM after DES pre-treatment, suggesting partial dissolution of crystal cellulose portions. For the packing in microfibril bundles, the detector data given in Fig. 7 were checked that all samples were placed vertically along the fibre direction, thus the extended scattering intensity in the horizontal axis compared to the vertical is due to the alignment of the microfibrils. The Organosolv and alkali pre-treatments do not significantly change the fibre orientation; the scattering is isotropic as in the raw chip. However, the DES treatment yields more isotropic scattering, confirming the loss of microfibril orientation due to the effective removal of the lignin and partial breakdown the cellular structure as also evidenced in SEM. Therefore, the weak form factor contribution in the DES-treated sample is due to the loss of crystallinity of the cellulose fibres and decrease of the packing order in the bundles. While previous studies have developed simple model fitting to SAXS data to reveal moisture-related structural changes in untreated wood samples (Penttilä et al., 2019), they are not readily applicable to the results presented in this work since the removal of lignin and hemicellulose was not accounted for in the early models. Nevertheless, the SAXS results reveal that different pre-treatment methods may result in distinct structural changes at the nanoscale, which ultimately affect the process efficiency and product quality.

3.3. *Influence of pre-treatment solvents on process techno-economics*

3.3.1. *Energy consumption*

Pre-treatment of LCB contributes approximately 40 % total cost of the overall biorefinery process (Wang and Lee, 2021). Although much research has investigated the use of various solvents in LCB pre-treatment in terms of the product yield and quality, there lacks practical knowledge of energy consumption and thus techno-economic impact of different pre-treatment methods, which hinders the process intensification and scale-up. In this work, we recorded the temperature and power profiles (temperature and/or power versus time) under microwave (from the Monowave software, an example is shown in supplementary material). In the microwave-assisted experimental setting, the sample mixture was firstly heated to the temperature of 120 °C under a constant power of 200 W (with all pre-treatments required similar a heating time of 0.5 – 1 min), after which it was kept at this temperature for set period of time while the microwave power was automatically tuned to between 0 – 15 W intermittently. The total energy usages (in kJ/g wood) were calculated as the sum of the area under the power profile and the results comparing three pre-treatments are shown in Fig. 8. The solvent properties of the three pre-treatments are listed in Table 1.

It is worth noting that the theoretical total energy (E_{Total}) is attributed to the sensible heat required to heat the biomass-solvent system (E_S) to the set temperature, any heat loss of the system (E_L) and efficiency of power conversion to heat (E_C), as shown in Eq. 6.

$$E_{Total} = E_S + E_L + E_C \quad (6)$$

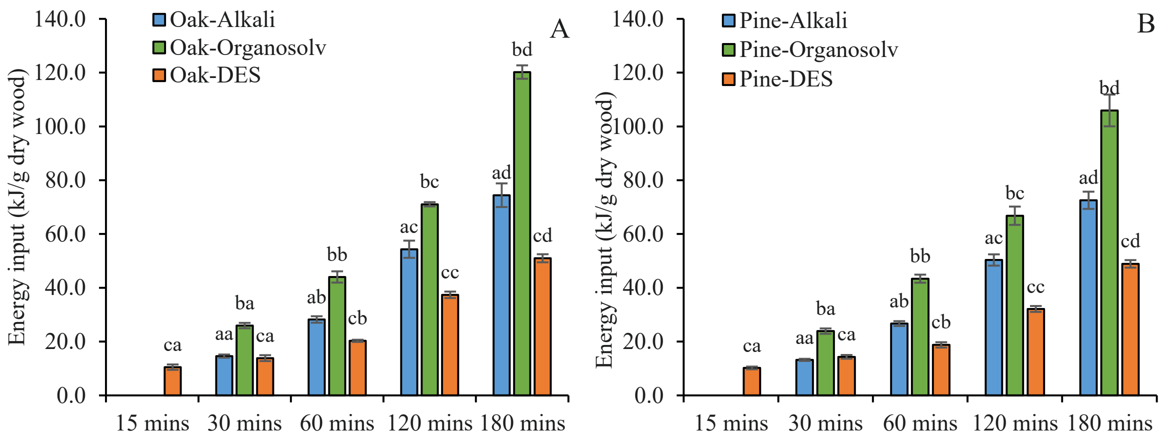

Fig. 8. Energy input requirement to process per gram of untreated wood by alkali, Organosolv and DES pre-treatment under microwaves (only considering the microwave heating step and excluding the downstream processes). (A). Oak wood; (B). Pine wood. Different letters in the same data figure indicate the significant difference ($p < 0.05$).

Table 1
Solvent property comparison of alkali, Organosolv and DES pre-treatments.

	Alkali pre-treatment	Organosolv pre-treatment	DES pre-treatment
Solvent composition	2.5 M NaOH and 0.4 M Na_2S	70 % ethanol with 1 % w/w H_2SO_4	PTSA: ChCl: Glycerol in 2:1:1 molar ratio
Boiling point (°C)	100 °C (for water)	78.9 °C	Higher than 120 °C
Saturated vapour pressure (bar)	2.0 bar (for water)	4.4 bar (for pure ethanol)	Negligible vapour pressure, liquid phase at 120 °C

In the presented experimental setting, the primary difference in energy consumption comparing the three pre-treatments is the E_S determined by the solvent heat capacities ($E_S = mCp\Delta T$), which are dependent on solvent types, temperature and system pressure, but the same regardless of the process scale and heating method. Results show that Organosolv has the highest energy consumption at almost twice the amount of DES (for example at 30 min time, 26.0 kJ/g oak wood for Organosolv pre-treatment than 13.9 kJ/g for DES; and similarly at 180 min, 120.2 kJ/g oak wood for Organosolv pre-treatment than 51.0 kJ/g for DES, Fig. 8, $p < 0.05$). This may be due to the high saturated vapour pressure (at approximately 4.4 bar, and low boiling point at approximately 78.9 °C, Table 1) of the Organoslv solution and thus higher energy consumption (higher enthalpy change) is required to hold the Organosolv solution at liquid phase at 120 °C. DES, on the contrary, is in liquid phase at the processing temperature and thus does not require pressurisation. On the other hand, E_L and E_C are intrinsic properties of the experimental systems and longer process time causes higher energy loss to the surrounding environment and through power conversion. Therefore, longer processing time requires higher energy consumption with approximately 4-fold increase from 30 min processing time to 180 min regardless of the pre-treatment types. Minimisation of heat loss can be achieved by better microwave cavity design and process insulation in scaled-up systems, so higher efficiency are generally expected compared with the laboratory scale systems (Mao et al., 2023b). At the tested conditions, the energy consumptions of DES pre-treatment are only 13.9 and 14.3 kJ/g for oak and pine respectively (120 °C, 30 min), while alkali pre-treatment requires 74.4 and 72.5 kJ/g for oak and pine perfectively (120 °C, 180 min), and Organosolv pre-treatment has the highest energy consumption at 120.2 and 105.9 kJ/g for oak and pine respectively (120 °C, 180 min) ($p < 0.05$).

However, since the above presented energy calculation was only collected under the studied experimental set-up and only considering the extraction/microwave heating step but excluding the downstream processes, the actual energy consumption in the industrial scale comparing the three pre-treatment methods may be notably different. The industrial energy efficiency is influenced by many factors including the scale of production, heating method (i.e. conventional heating vs microwave heating), process conditions, downstream processes and solvent/energy recycle and reuse. However, most of the currently available energy information on biomass delignification is limited to the Kraft process, as this is an already established commercial process; there is some information regarding the Organosolv process (Rabelo et al., 2023), but no existing information on DES process. Additionally, discussion of energy consumption in the literature is limited to conventional rather than microwave heating, which is still novel in industrial implementation. This work therefore provides useful information on the energy requirements for the microwave-assisted pre-treatment process for the first time, supporting preliminary techno-economic analysis of novel biomass pre-treatment processes.

3.3.2. Implications on process techno-economics

Understanding the impacts of different pre-treatment methods and solvent systems on process techno-economics requires consideration of various aspects:

- Solvent sustainability and tailorability: Some DES and organic solvents can be green, environmentally-friendly and no/low toxicity. For example, natural deep eutectic solvents (NADES) can be derived from natural sources and some could be food grade and biodegradable (e.g. choline chloride (ChCl), glycerol (Gly), carbohydrates, urea, polyalcohols, lactic acid, amino acids and vitamins etc.) (del Mar Contreras-Gámez et al., 2023; Perna et al., 2020), although not the DES studied in this work. The high alkalinity solvent used in conventional industrial lignin removal, i.e. the Kraft process, often requires appropriate treatment such as neutralisation before disposal to the environment. Unlike DES and Organosolv processes, which show high process tailorability towards targeted biorefinery applications through various solvent selections, Kraft process is often limited to the use of sodium hydroxide and sodium sulphide (Perna et al., 2020).
- Solvent cost and recyclability: Alkali solvents currently offer the lowest cost compared to the DES and organic solvents. The cost of DES could be reduced through the selection of relatively low-cost and solid chemical components, which allows easier storage and shipping, and can be prepared on site by mixing of the components with moderate heating (Tomé et al., 2018). Recovery and recycling of the pre-treatment solvents, which are most commonly achieved by

evaporation of the water content in the spent solvents, can potentially further reduce the solvent cost; however, it brings additional investment and running cost of the evaporation unit and further techno-economic analysis is required to enable robust comparison of the different options. Some constituents in the DES (such as choline chloride) can also be partially recovered by recrystallisation using anti-solvent (Isci and Kaltschmitt, 2021), which is a less energy-intensive process than evaporation; however, the research on DES recovery efficiency is still limited and future work is required to understand the recyclability of DES compared with the other traditional and organic solvents. Solvent recycling is currently a major barrier to scale-up of DES extraction processes.

- Downstream process and overall process energy requirement: The results presented in Section 3.3.1 indicate that the shorter processing times required for DES pre-treatment compared with alkali and Organosolv pre-treatments lead to significantly lower energy requirements (1/5–1/8 compared with alkali and Organosolv pre-treatments respectively at laboratory scale). However, further understanding of the downstream processes (i.e. product separation and purification, lignin precipitation) and thus overall process energy is required. Modern Kraft pulp mills have a complete recovery cycle, in which energy from the combustion of the dissolved lignin and the pulping chemicals in the black liquor are recovered simultaneously, making it self-sufficient in energy and meet all internal steam and electricity demand for the process (Naqvi et al., 2010). The future commercialisation of Oragnosolv and DES process is likely to integrate this established downstream unit and recovery cycle operations. In the meantime, emerging research is currently driving advances in lignin and hemicellulose valorisation, which is hoped to produce products with higher value applications, therefore increasing the economic benefits of the pulping biorefinery.
- Process unit requirement: Both alkali and Organosolv processes require pressurised systems, and the latter also has fire hazards. Conversely, the DES process offers atmospheric pressure operation and non-flammable process streams with high chemical and thermal stability. Alkali pre-treatment could lead to extra costs relating to corrosion prevention and effective disposal of the solvent. Due to the much higher viscosity and density of DES (690 mPa·s and 1.8 g/mL for the studied DES at room temperature), DES process poses challenges in industrial scale-up and is likely require a lower biomass-to-solvent ratio than the Kraft/alkali and Organosolv processes to enable a flow system design and product separation. DES remains associated with biomass after common product purification practices such as alcohol and/or water washing, and therefore poses challenges to the downstream process. In this study, we used dialysis for extensive product purification, which was the most time-consuming step (5 days) in our methodology and its usage in large-scale industrial manufacturing is challenging and costly. Another possible solution is adding a small amount of water to the DES (namely hydrated-DES system) to decrease its viscosity and increase solubility in washing solvents, which however, in turn may compromise the chemical (e.g. intermolecular bonding structure) and physical (increased vapour pressure) properties of the original DES (Gygli et al., 2020). Knowledge on the effects and optimum content of the adding water to LCB fractionation is still insufficient and future work is required. Although the present study proves the benefits of the unique selective and instant heating offered by the microwaves to overcome its heat and mass transfer limitations and reduce the process time, the scaling up of a microwave-assisted heating process may be expensive in capital cost due to the large capital investment for microwave generator (Dewi et al., 2024).

3.4. Study limitations and future perspectives

The novelty of this study is the systematic comparison of the alkali, organsolv and DES pre-treatments addressing the knowledge gaps in sustainable solvent selections in biorefinery. This is the first experimental comparison of the three pre-treatment methods with all variables controlled (i.e. time, temperature, heating mechanism (microwave heating), biomass type, biomass to solvent ratio etc.). While this study provides insights at the laboratory set-ups, some of the process conditions presented may not align with existing industrial practices, limiting the direct applicability of the results to industrial-scale scenarios (such as industrial Kraft process). Specific limitations of this study are discussed below:

- Solvent selection is not fully representative: Only one solvent was selected representing each pre-treatment method category, while it should be acknowledged that different chemical compositions of solvents (for example, different compositions of the alkali solvents, different types of organic solvents and compositions in water, different selections of HBA and HBD and their molar ratios in DES) also have significant impact on the pre-treatment (Bao et al., 2024; Wang et al., 2024). The concentration of the alkali solution used in this study does not fully represent the industrial Kraft process, where NaOH and Na_2S at concentrations of 15–20 % are commonly used (Pola et al., 2022; Woiciechowski et al., 2020). Future work should elucidate the susceptibility of a wider range of solvents and the influence of solvent compositions to biomass fractionation.
- Operating conditions are not optimised: The extraction temperature and time used in the present study (120 °C, up to 180 min) was selected based on the preliminary optimisation of DES process, but it is not the optimised temperature for alkali and Organosolv processes where temperatures above 150 °C and longer time are usually reported in the literature (Liu et al., 2020; Parot et al., 2022). Future work is required to elucidate the influence of various operating conditions, such as temperature and time. The size of the raw wood studied was much reduced compared with industrial practices and the influence of biomass sizes on pre-treatment efficiency and techno-economic on grinding and separation steps are not considered. The biomass-to-solvent ratio studied (1:20), although within the range of commonly-reported laboratory set-ups (Liu et al., 2020; Mao et al., 2023a; Parot et al., 2022; Xie et al., 2023) is much higher than the industrial processes (which is typically between 1:3.5–1:5). Future work should elucidate the process optimisation and intensification using conditions more representative of the industrial process.
- Feedstock selection is limited: Only two biomass samples (an oak and a pine wood) were selected as the study material to present the two major lignocellulose types (hardwood and softwood, respectively); while future work on a wider range of industrial-relevant LCB is required.
- Other valuable by-products (i.e. lignin and hemicellulose) are not studied: The presented work focuses particularly on the cellulose-rich fraction (CRF, solid fraction after the pre-treatments), although lignin recovery was also mentioned, its detailed characterisation is outside the scope. Emerging research has demonstrated the potential of lignin in several advanced material applications, including bioplastics, biosurfactant, and hydrogels with antimicrobial and antioxidant properties etc. (Rico-García et al., 2020; Sethupathy et al., 2022; Xia et al., 2021). Literature has also paid little attention to date to the hemicellulose that is dissolved in the pre-treatment solvents. Hemicellulose undergoes continuous degradation and becomes less recoverable due to reduced molecular weight, posing a major barrier to solvent recycling (Chen et al., 2022). Future work is required to further the study of lignin valorisation and hemicellulose recovery using different pre-treatments, hoping to deepen the understanding in LCB biorefinery and fulfil the Circular Economy Concepts.

4. Conclusion

An alkali, Organosolv and DES pre-treatments were systematically compared to understand their influences on biomass compositional and structural alterations on both oak and pine wood. Delignification yields and energy consumptions were compared to understand the process efficiency and provide preliminary techno-economic comparison of the three pre-treatment methods. Complementary characterisation of the treated wood shows varied physiochemical properties between different pre-treatments, informing product susceptibility for different upgrading routes. While the presented comparison brings insights at the laboratory set-up, future work is required to achieve process optimisation under industrial-relevant conditions to maximise the result applicability for industrial scale-ups. Future work is also required on recovered lignin by-product development, hemicellulose recovery and solvent recycling to fulfil the Circular Economy Concept in the biorefinery.

CRediT authorship contribution statement

Senses Erkan: Writing – review & editing, Writing – original draft, Supervision, Resources, Project administration, Methodology, Investigation, Funding acquisition, Conceptualization. **Lee Chai Siah:** Investigation, Formal analysis. **Oven Gwyn:** Investigation, Formal analysis. **Tarhanli Ilayda:** Methodology, Investigation, Formal analysis, Conceptualization. **Mao Yujie:** Writing – review & editing, Writing – original draft, Visualization, Validation, Methodology, Investigation, Formal analysis, Conceptualization. **Binner Eleanor R:** Writing – review & editing, Supervision, Resources, Funding acquisition, Conceptualization.

Declaration of Competing Interest

The authors declare that they have no known competing financial interests or personal relationships that could have appeared to influence the work reported in this paper.

Acknowledgements

This work was supported by TÜBİTAK-Royal Academy of Engineering Transforming Systems for Partnership Program [grant number 220N257] and TÜBİTAK 1001 Program [grant number: 222Z106]. The authors acknowledge the use of SAXS services and facilities of n2STAR-KU Nanofabrication and Nanocharacterization Center for Scientific and Technological Advanced Research. We thank Dr. Barış Yağcı of KU Center for Surface Science and Technology for SEM images. We would like to acknowledge Gülşah Balamut and Başak Bengü from Kastamonu Entegre (KEAS) for providing the raw oak and pine chips.

Appendix A. Supporting information

Supplementary data associated with this article can be found in the online version at doi:10.1016/j.indcrop.2025.120614.

Data Availability

Data will be made available on request.

References

Alvarez-Vasco, C., Ma, R., Quintero, M., Guo, M., Geleynse, S., Ramasamy, K.K., Wolcott, M., Zhang, X., 2016. Unique low-molecular-weight lignin with high purity extracted from wood by deep eutectic solvents (DES): a source of lignin for valorization. Green. Chem. 18, 5133–5141. https://doi.org/10.1039/C6GC01007E.

Ashokkumar, V., Venkatkarthick, R., Jayashree, S., Chuetor, S., Dharmaraj, S., Kumar, G., Chen, W.-H., Ngamcharussrivichai, C., 2022. Recent advances in lignocellulosic biomass for biofuels and value-added bioproducts-a critical review. Bioresour. Technol. 344, 126195. https://doi.org/10.1016/j.biortech.2021.126195.

Bailey, R.W., 1958. The reaction of pentoses with anthrone. Biochem. J. 68, 669. https://doi.org/10.1042/bj0680669.

Bao, Y., Wang, Y., Yan, C., Xue, Z., 2024. Deep eutectic solvents for fractionation and valorization of lignocellulose. Green. Chem. Eng. 6, 21–35. https://doi.org/10.1016/j.gce.2024.04.001.

Barnes, W.J., Anderson, C.T., 2017. Acetyl bromide soluble lignin (ABSL) assay for total lignin quantification from plant biomass. e2149 Bio-Protoc. 7, e2149. https://doi.org/10.21769/BioProtoc.2149.

Bensidhom, G., Hassen-Trabelsi, A.B., Alper, K., Sghairoun, M., Zaafouri, K., Trabelsi, I., 2018. Pyrolysis of Date palm waste in a fixed-bed reactor: characterization of pyrolytic products. Bioresour. Technol. 247, 363–369. https://doi.org/10.1016/j.biortech.2017.09.066.

Ceaser, R., Rosa, S., Montané, D., Constantí, M., Medina, F., 2023. Optimization of softwood pretreatment by microwave-assisted deep eutectic solvents at high solids loading. Bioresour. Technol. 369, 128470. https://doi.org/10.1016/j.biortech.2022.128470.

Chen, H., Liu, Z., Chen, X., Chen, Y., Dong, Z., Wang, X., Yang, H., 2020. Comparative pyrolysis behaviors of stalk, wood and shell biomass: correlation of cellulose crystallinity and reaction kinetics. Bioresour. Technol. 310, 123498. https://doi.org/10.1016/j.biortech.2020.123498.

Chen, Z., Wang, Y., Cheng, H., Zhou, H., 2022. Hemicellulose degradation: an overlooked issue in acidic deep eutectic solvents pretreatment of lignocellulosic biomass. Ind. Crops Prod. 187, 115335. https://doi.org/10.1016/j.indcrop.2022.115335.

Chio, C., Sain, M., Qin, W., 2019. Lignin utilization: a review of lignin depolymerization from various aspects. Renew. Sustain. Energy Rev. 107, 232–249. https://doi.org/10.1016/j.rser.2019.03.008.

Debnath, B., Haldar, D., Purkait, M.K., 2021. A critical review on the techniques used for the synthesis and applications of crystalline cellulose derived from agricultural wastes and forest residues. Carbohydr. Polym. 273, 118537. https://doi.org/10.1016/j.carbpol.2021.118537.

Devi, A., Bajar, S., Kour, H., Kothari, R., Pant, D., Singh, A., 2022. Lignocellulosic biomass valorization for bioethanol production: a circular bioeconomy approach. Bioenergy Res. 15, 1820–1841. https://doi.org/10.1007/s12155-022-10401-9.

Dewi, S.R., Stevens, L.A., Anwar, M., Mao, Y., Ferrari, R.S., Irvine, D.J., Binner, E.R., 2024. Towards a scalable cacao pod husk biorefinery: understanding the effects of process conditions on phenolic antioxidant extraction and residual solid properties. Chem. Eng. Sci., 121171 https://doi.org/10.1016/j.ces.2024.121171.

González-Rivera, J., Husanu, E., Mero, A., Ferrari, C., Duce, C., Tinè, M.R., D'Andrea, F., Pomelli, C.S., Guazzelli, L., 2020. Insights into microwave heating response and thermal decomposition behavior of deep eutectic solvents. J. Mol. Liq. 300, 112357. https://doi.org/10.1016/j.molliq.2019.112357.

Gygli, G., Xu, X., Pleiss, J., 2020. Meta-analysis of viscosity of aqueous deep eutectic solvents and their components. Sci. Rep. 10, 21395. https://doi.org/10.1038/s41598-020-78101-y.

Haq, I., Mazumder, P., Kalamdhad, A.S., 2020. Recent advances in removal of lignin from paper industry wastewater and its industrial applications–a review. Bioresour. Technol. 312, 123636. https://doi.org/10.1016/j.biortech.2020.123636.

Hattori, K., Arai, A., 2016. Preparation and hydrolysis of water-stable amorphous cellulose. ACS Sustain. Chem. Eng. 4, 1180–1186. https://doi.org/10.1021/acssuschemeng.5b01247.

Hoang, A.T., Ong, H.C., Fattah, I.R., Chong, C.T., Cheng, C.K., Sakthivel, R., Ok, Y.S., 2021. Progress on the lignocellulosic biomass pyrolysis for biofuel production toward environmental sustainability. Fuel Process. Technol. 223, 106997. https://doi.org/10.1016/j.fuproc.2021.106997.

Isci, A., Kaltschmitt, M., 2021. Recovery and recycling of deep eutectic solvents in biomass conversions: a review. Biomass. Convers. Biorefinery 12, 197–226. https://doi.org/10.1007/s13399-021-01860-9.

Kohli, K., Katuwal, S., Biswas, A., Sharma, B.K., 2020. Effective delignification of lignocellulosic biomass by microwave assisted deep eutectic solvents. Bioresour. Technol. 303, 122897. https://doi.org/10.1016/j.biortech.2020.122897.

Kumar, A., Kumar, J., Bhaskar, T., 2020. Utilization of lignin: a sustainable and eco-friendly approach. J. Energy Inst. 93, 235–271. https://doi.org/10.1016/j.joei.2019.03.005.

Kumar, A.K., Sharma, S., 2017. Recent updates on different methods of pretreatment of lignocellulosic feedstocks: a review. Bioresour. Bioprocess. 4, 1–19. https://doi.org/10.1186/s40643-017-0137-9.

Kumar, V., Binod, P., Sindhu, R., Gnansounou, E., Ahluwalia, V., 2018. Bioconversion of pentose sugars to value added chemicals and fuels: recent trends, challenges and possibilities. Bioresour. Technol. 269, 443–451. https://doi.org/10.1016/j.biortech.2018.08.042.

Lahtinen, M.H., Mikkila, J., Mikkonen, K.S., Kilpelainen, I., 2021. Kraft Process—formation of secoisolariciresinol structures and incorporation of fatty acids in Kraft Lignin. J. Agric. Food Chem. 69, 5955–5965. https://doi.org/10.1021/acs.jafc.1c00705.

Liao, J.J., Abd Latif, N.H., Trache, D., Brosse, N., Hussin, M.H., 2020. Current advancement on the isolation, characterization and application of lignin. Int. J. Biol. Macromol. 162, 985–1024. https://doi.org/10.1016/j.ijbiomac.2020.06.168.

Liu, L.-Y., Patankar, S.C., Chandra, R.P., Sathitsuksanoh, N., Saddler, J.N., Renneckar, S., 2020. Valorization of bark using ethanol–water organosolv treatment: isolation and characterization of crude lignin. ACS Sustain. Chem. Eng. 8, 4745–4754. https://doi.org/10.1021/acssuschemeng.9b06692.

Lobato-Rodríguez, Á., Gullón, B., Romaní, A., Ferreira-Santos, P., Garrote, G., Del-Río, P. G., 2023. Recent advances in biorefineries based on lignin extraction using deep eutectic solvents: a review. Bioresour. Technol., 129744 https://doi.org/10.1016/j.biortech.2023.129744.

Loix, C., Huybrechts, M., Vangronsveld, J., Gielen, M., Keunen, E., Cuypers, A., 2017. Reciprocal interactions between cadmium-induced cell wall responses and oxidative stress in plants. Front. Plant Sci. 8, 1867. https://doi.org/10.3389/fpls.2017.01867.

Lu, Y., Lu, Y.-C., Hu, H.-Q., Xie, F.-J., Wei, X.-Y., Fan, X., 2017. Structural characterization of lignin and its degradation products with spectroscopic methods. J. Spectrosc. 2017, 8951658. https://doi.org/10.1155/2017/8951658.

Luo, H., Abu-Omar, M.M., 2018. Lignin extraction and catalytic upgrading from genetically modified poplar. Green. Chem. 20, 745–753. https://doi.org/10.1039/C7GC03417B.

Maia, R.A., Ventorim, G., Batagin-Neto, A., 2019. Reactivity of lignin subunits: the influence of dehydrogenation and formation of dimeric structures. J. Mol. Model. 25, 228. https://doi.org/10.1007/s00894-019-4130-4.

Mao, Y., Robinson, J., Binner, E., 2021. Understanding heat and mass transfer processes during microwave-assisted and conventional solvent extraction. Chem. Eng. Sci. 233, 116418. https://doi.org/10.1016/j.ces.2020.116418.

Mao, Y., Gerrow, A., Ray, E., Perez, N.D., Edler, K., Wolf, B., Binner, E., 2023a. Lignin recovery from cocoa bean shell using microwave-assisted extraction and deep eutectic solvents. Bioresour. Technol. 372, 128680. https://doi.org/10.1016/j.biortech.2023.128680.

Mao, Y., Robinson, J.P., Binner, E.R., 2023b. Current status of microwave-assisted extraction of pectin. Chem. Eng. J., 145261 https://doi.org/10.1016/j.cej.2023.145261.

del Mar Contreras-Gámez, M., Galán-Martín, Á., Seixas, N., da Costa Lopes, A.M., Silvestre, A., Castro, E., 2023. Deep eutectic solvents for improved biomass pretreatment: current status and future prospective towards sustainable processes. Bioresour. Technol. 369, 128396. https://doi.org/10.1016/j.biortech.2022.128396.

Mierzwa-Hersztek, M., Gondek, K., Jewiarz, M., Dziedzic, K., 2019. Assessment of energy parameters of biomass and biochars, leachability of heavy metals and phytotoxicity of their ashes. J. Mater. Cycles Waste Manag. 21, 786–800. https://doi.org/10.1007/s10163-019-00832-6.

Naqvi, M., Yan, J., Dahlquist, E., 2010. Black liquor gasification integrated in pulp and paper mills: a critical review. Bioresour. Technol. 101, 8001–8015. https://doi.org/10.1016/j.biortech.2010.05.013.

Ning, P., Yang, G., Hu, L., Sun, J., Shi, L., Zhou, Y., Wang, Z., Yang, J., 2021. Recent advances in the valorization of plant biomass. Biotechnol. Biofuels 14, 102. https://doi.org/10.1186/s13068-021-01949-3.

Nitsos, C., Stoklosa, R., Karnaouri, A., Voros, D., Lange, H., Hodge, D., Crestini, C., Rova, U., Christakopoulos, P., 2016. Isolation and characterization of organosolv and alkaline lignins from hardwood and softwood biomass. ACS Sustain. Chem. Eng. 4, 5181–5193. https://doi.org/10.1021/acssuschemeng.6b01205.

Ouyang, X., Huang, X., Hendriks, B.M., Boot, M.D., Hensen, E.J., 2018. Coupling organosolv fractionation and reductive depolymerization of woody biomass in a two-step catalytic process. Green. Chem. 20, 2308–2319. https://doi.org/10.1039/C8GC00639C.

Parot, M., Rodrigue, D., Stevanovic, T., 2022. High purity softwood lignin obtained by an eco-friendly organosolv process. Bioresour. Technol. Rep. 17, 100880. https://doi.org/10.1016/j.biteb.2021.100880.

Patil, S.S., Rathod, V.K., 2023. Extraction and purification of curcuminoids from Curcuma longa using microwave assisted deep eutectic solvent based system and cost estimation. Process Biochem. 126, 61–71. https://doi.org/10.1016/j.procbio.2022.11.010.

Penttilä, P.A., Rautkari, L., Österberg, M., Schweins, R., 2019. Small-angle scattering model for efficient characterization of wood nanostructure and moisture behaviour. J. Appl. Crystallogr. 52, 369–377. https://doi.org/10.1107/S1600576719002012.

Penttilä, P.A., Altgen, M., Carl, N., van Der Linden, P., Morfin, I., Österberg, M., Schweins, R., Rautkari, L., 2020. Moisture-related changes in the nanostructure of woods studied with X-ray and neutron scattering. Cellulose 27, 71–87. https://doi.org/10.1007/s10570-019-02781-7.

Perna, F.M., Vitale, P., Capriati, V., 2020. Deep eutectic solvents and their applications as green solvents. Curr. Opin. Green. Sustain. Chem. 21, 27–33. https://doi.org/10.1016/j.cogsc.2019.09.004.

Pola, L., Collado, S., Oulego, P., Díaz, M., 2022. Kraft black liquor as a renewable source of value-added chemicals. Chem. Eng. J. 448, 137728. https://doi.org/10.1016/j.cej.2022.137728.

Rabelo, S.C., Nakasu, P.Y.S., Scopel, E., Araújo, M.F., Cardoso, L.H., da, Costa, A.C., 2023. Organosolv pretreatment for biorefineries: current status, perspectives, and challenges. Bioresour. Technol. 369, 128331. https://doi.org/10.1016/j.biortech.2022.128331.

Rahman, M.M., Payel, M.T.H., Asaduzzaman, M., Hossain, S., Ali, M., 2024. Physical properties of isolated cellulose fiber from jute and banana fiber through kraft pulping: potential applications in packaging and regenerated fibers. SPE Polym. 5, 709–717. https://doi.org/10.1002/pls2.10155.

Rico-García, D., Ruiz-Rubio, L., Pérez-Alvarez, L., Hernández-Olmos, S.L., Guerrero-Ramírez, G.L., Vilas-Vilela, J.L., 2020. Lignin-based hydrogels: synthesis and applications. Polymers 12, 81. https://doi.org/10.3390/polym12010081.

Sankhla, S., Sardar, H.H., Neogi, S., 2021. Greener extraction of highly crystalline and thermally stable cellulose micro-fibers from sugarcane bagasse for cellulose nanofibrils preparation. Carbohydr. Polym. 251, 117030. https://doi.org/10.1016/j.carbpol.2020.117030.

Sarıoğlu, E., Tarhanlı, İ., Yarıcı, T., Bengü, B., Erkey, C., Senses, E., 2025. Unraveling the effects of cellulose nanoparticle types on dispersion, rheological behavior, and shear strength in adhesive formulations. Carbohydr. Polym., 123261 https://doi.org/10.1016/j.carbpol.2025.123261.

Sathawong, S., Sridach, W., Techato, K.-a, 2018. Lignin: Isolation and preparing the lignin based hydrogel. J. Environ. Chem. Eng. 6, 5879–5888. https://doi.org/10.1016/j.jece.2018.05.008.

Sethupathy, S., Morales, G.M., Gao, L., Wang, H., Yang, B., Jiang, J., Sun, J., Zhu, D., 2022. Lignin valorization: status, challenges and opportunities. Bioresour. Technol. 347, 126696. https://doi.org/10.1016/j.biortech.2022.126696.

Sirviö, J.A., Mikola, M., Ahola, J., Heiskanen, J.P., Filonenko, S., Ämmälä, A., 2023. Highly effective fractionation chemistry to overcome the recalcitrance of softwood lignocellulose. Carbohydr. Polym. 312, 120815. https://doi.org/10.1016/j.carbpol.2023.120815.

Stamogiannou, I., Van Camp, J., Smagghe, G., Van de Walle, D., Dewettinck, K., Raes, K., 2021. Impact of phenolic compound as activators or inhibitors on the enzymatic hydrolysis of cellulose. Int. J. Biol. Macromol. 186, 174–180. https://doi.org/10.1016/j.ijbiomac.2021.07.052.

Sumerskii, I., Zweckmair, T., Hettegger, H., Zinovyev, G., Bacher, M., Rosenau, T., Potthast, A., 2017. A fast track for the accurate determination of methoxyl and ethoxyl groups in lignin. RSC Adv. 7, 22974–22982. https://doi.org/10.1039/C7RA00690J.

Tarhanlı, İ., Senses, E., 2023. Cellulose nanocrystal and Pluronic L121-based thermo-responsive composite hydrogels. Carbohydr. Polym. 321, 121281. https://doi.org/10.1016/j.carbpol.2023.121281.

Tomé, L.I., Baião, V., da Silva, W., Brett, C.M., 2018. Deep eutectic solvents for the production and application of new materials. Appl. Mater. Today 10, 30–50. https://doi.org/10.1016/j.apmt.2017.11.005.

Vidal, G., González, Y., Piña, B., Jarpa, M., Gómez, G., 2021. Minimization of environmental impact of kraft pulp mill effluents: current practices and future perspectives towards sustainability. Sustainability 13, 9288. https://doi.org/10.3390/su13169288.

Wang, N., Xu, A., Liu, K., Zhao, Z., Li, H., Gao, X., 2024. Performance of green solvents in microwave-assisted pretreatment of lignocellulose. Chem. Eng. J. 482, 148786. https://doi.org/10.1016/j.cej.2024.148786.

Wang, W., Lee, D.-J., 2021. Lignocellulosic biomass pretreatment by deep eutectic solvents on lignin extraction and saccharification enhancement: a review. Bioresour. Technol. 339, 125587. https://doi.org/10.1016/j.biortech.2021.125587.

Wei, W., Wang, B., Wang, X., Ling, R., Jin, Y., 2021. Comparison of acid and alkali catalyzed ethylene glycol organosolv pretreatment for sugar production from bagasse. Bioresour. Technol. 320, 124293. https://doi.org/10.1016/j.biortech.2020.124293.

Woiciechowski, A.L., Neto, C.J.D., de Souza Vandenberghe, L.P., de Carvalho Neto, D.P., Sydney, A.C.N., Letti, L.A.J., Karp, S.G., Torres, L.A.Z., Soccol, C.R., 2020. Lignocellulosic biomass: acid and alkaline pretreatments and their effects on biomass recalcitrance–Conventional processing and recent advances. Bioresour. Technol. 304, 122848. https://doi.org/10.1016/j.biortech.2020.122848.

Xia, Q., Chen, C., Yao, Y., Li, J., He, S., Zhou, Y., Li, T., Pan, X., Yao, Y., Hu, L., 2021. A strong, biodegradable and recyclable lignocellulosic bioplastic. Nat. Sustain. 4, 627–635. https://doi.org/10.1038/s41893-021-00702-w.

Xie, Y., Zhao, J., Wang, P., Ling, Z., Yong, Q., 2023. Natural arginine-based deep eutectic solvents for rapid microwave-assisted pretreatment on crystalline bamboo cellulose with boosting enzymatic conversion performance. Bioresour. Technol. 385, 129438. https://doi.org/10.1016/j.biortech.2023.129438.

Xu, H., Che, X., Ding, Y., Kong, Y., Li, B., Tian, W., 2019. Effect of crystallinity on pretreatment and enzymatic hydrolysis of lignocellulosic biomass based on multivariate analysis. Bioresour. Technol. 279, 271–280. https://doi.org/10.1016/j.biortech.2018.12.096.

Yang, H., Yan, R., Chen, H., Lee, D.H., Zheng, C., 2007. Characteristics of hemicellulose, cellulose and lignin pyrolysis. Fuel 86, 1781–1788. https://doi.org/10.1016/j.fuel.2006.12.013.

Yu, H., Gui, C., Ji, Y., Li, X., Rao, F., Huan, W., Li, L., 2022. Changes in chemical and thermal properties of bamboo after delignification treatment. Polymers 14, 2573. https://doi.org/10.3390/polym14132573.

Zhang, L., Larsson, A., Moldin, A., Edlund, U., 2022. Comparison of lignin distribution, structure, and morphology in wheat straw and wood. Ind. Crops Prod. 187, 115432. https://doi.org/10.1016/j.indcrop.2022.115432.

Zou, R., Zhou, X., Qian, M., Wang, C., Boldor, D., Lei, H., Zhang, X., 2023. Advancements and applications of microwave-assisted deep eutectic solvent (MW-DES) lignin extraction: a comprehensive review. Green. Chem. https://doi.org/10.1039/D3GC04501C.